Journal of Mathematical Biology (2024) 88:45
https://doi.org/10.1007/s00285-024-02068-x

Mathematical Biology

Mutations make pandemics worse or better: modeling SARS-CoV-2 variants and imperfect vaccination

Sarita Bugalia[1] · Jai Prakash Tripathi[1] · Hao Wang[2]

Received: 30 December 2021 / Revised: 4 July 2023 / Accepted: 18 February 2024 /
Published online: 20 March 2024
© The Author(s), under exclusive licence to Springer-Verlag GmbH Germany, part of Springer Nature 2024

Abstract

COVID-19 is a respiratory disease triggered by an RNA virus inclined to mutations. Since December 2020, variants of COVID-19 (especially Delta and Omicron) continuously appeared with different characteristics that influenced death and transmissibility emerged around the world. To address the novel dynamics of the disease, we propose and analyze a dynamical model of two strains, namely native and mutant, transmission dynamics with mutation and imperfect vaccination. It is also assumed that the recuperated individuals from the native strain can be infected with mutant strain through the direct contact with individual or contaminated surfaces or aerosols. We compute the basic reproduction number, R_0, which is the maximum of the basic reproduction numbers of native and mutant strains. We prove the nonexistence of backward bifurcation using the center manifold theory, and global stability of disease-free equilibrium when $R_0 < 1$, that is, vaccine is effective enough to eliminate the native and mutant strains even if it cannot provide full protection. Hopf bifurcation appears when the endemic equilibrium loses its stability. An intermediate mutation rate ν_1 leads to oscillations. When ν_1 increases over a threshold, the system regains its stability and exhibits an interesting dynamics called endemic bubble. An analytical expression for vaccine-induced herd immunity is derived. The epidemiological implication of the herd immunity threshold is that the disease may effectively be eradicated if the minimum herd immunity threshold is attained in the community. Furthermore, the model is parameterized using the Indian data of the cumulative number of confirmed cases and deaths of COVID-19 from March 1 to September 27 in 2021, using MCMC method. The cumulative cases and deaths can be reduced by increasing the vaccine efficacies to both native and mutant strains. We observe that by considering the vac-

✉ Jai Prakash Tripathi
jtripathi85@gmail.com

[1] Department of Mathematics, Central University of Rajasthan, Bandar Sindri, Kishangarh, Ajmer, Rajasthan 305817, India

[2] Department of Mathematical and Statistical Sciences, University of Alberta, Edmonton, AB T6G 2G1, Canada

cine efficacy against native strain as 90%, both cumulative cases and deaths would be reduced by 0.40%. It is concluded that increasing immunity against mutant strain is more influential than the vaccine efficacy against it in controlling the total cases. Our study demonstrates that the COVID-19 pandemic may be worse due to the occurrence of oscillations for certain mutation rates (i.e., outbreaks will occur repeatedly) but better due to stability at a lower infection level with a larger mutation rate. We perform sensitivity analysis using the Latin Hypercube Sampling methodology and partial rank correlation coefficients to illustrate the impact of parameters on the basic reproduction number, the number of cumulative cases and deaths, which ultimately sheds light on disease mitigation.

Keywords COVID-19 · Endemic bubble · Mutation · Imperfect vaccination · MCMC · Two strain dynamics · Hopf bifurcation · Transcritical bifurcation · Sensitivity analysis

Mathematics Subject Classification 92D30 · 34D23 · 34K18 · 34C10

1 Introduction

Contagious diseases are one of the foremost reasons for demise worldwide. The spread of contagious diseases dangerously affects the growth of countries and the evolution of a population. Though modern scientific medicine has made rapid advancements, the diseases have not been completely eradicated. Diseases have obtained new versions due to the genetic variations of pathogens triggered via mutations. Many pathogens are characterized by more than one variant (Sato et al. 1995; Palese and Young 1982). Virus or pathogen mutations are general in contagious diseases such as HBV (Sato et al. 1995), influenza (Palese and Young 1982), and HIV (Eron et al. 1998). Multiple strains of the 1918 avian influenza virus with mutations have been recognized by Iwami et al. (2007). The existence of different variants of a pathogen is mainly due to resist immune attacks of the host or induced by treatment with antiviral drugs or antibodies (Eron et al. 1998). Ultimately, they confirm the persistence of disease in a host. Sansonetti and Arondel (1989) have revealed that mutant strains can be associated with higher virulence to disease than the native strains, and those people diseased with mutant strains have a higher death rate in the contagious diseases, such as plague, influenza A, etc. Thus, one of the major challenges in stopping the spread of infectious diseases is to treat the genetic variations of pathogens (May and Nowak 1995; Parton et al. 1994; Liu et al. 2018). Various epidemic models with multi-strain contacts and mutations have been proposed in recent years from different aspects (Liu et al. 2018; Cai et al. 2012; Li et al. 2004). Li et al. (2004) proposed a two-strain SIR model with infection age and mutation. The authors analyzed the local and global stability of all possible equilibria and Hopf bifurcation. Liu et al. (2018) proposed a mathematical model for Influenza with virus mutation and analyzed the model in the sense of permanence of the disease. Moreover, epidemiological investigations have exposed that the phenomenon of mutations leads to further resistant viruses giving the emergence of many new dangerous epidemics or even new serious pandemics.

Since December 2019, a new coronavirus causing a respiratory disease known as COVID-19 has rapidly spread and affected a large portion of the global population. The World Health Organization (WHO) has detected the spread of COVID-19 as a pandemic, and as of December 4, 2021, over 263 million people were diseased, and about 5.2 million deaths caused by the virus. The SARS-CoV-2 virus triggered by severe acute respiratory syndrome is also mutating. Lately, numerous variants of the SARS-CoV-2 virus have been identified. These variants are described according to the number and types of mutations (Korber et al. 2020; Lemieux and Li 2021). At the beginning of the COVID-19 pandemic, the SARS-CoV-2 coronavirus that initiated COVID-19 has mutated, raising different variants of the virus. Numerous SARS-CoV-2 variants have developed worldwide, and the presence of different variants depends on several factors. One of these is called the delta variant, which was first identified in India (Centers for Disease Control and Prevention (CDC) 2021a). Different variants have appeared in Brazil, England, California, and other countries. More transmittable variants such as beta, which was primarily emerged in South Africa, may have improved the ability to re-infect individuals who have recuperated from previous versions of the virus and also be somewhat resistant to some of the coronavirus vaccines in development (Johns Hopkins Medicine 2021). These new variants might have distinct features that can influence the death rate and transmissibility (Korber et al. 2020; Lemieux and Li 2021; Gonzalez-Parra et al. 2021). From October 2020, the number of infected cases of SARS-CoV-2 and related deaths augmented drastically in England. It has been discovered that the new SARS-CoV-2 variant VOC-202012/01 was widespread, and its proportion amplified throughout the latest months in England (Bussiness Insider 2021; Public Health England 2021). The mutations of viruses are frequent, and as an outcome, SARS-CoV-2 may develop mutations with immunological resistance and fitness advantages (Korber et al. 2020). It is anticipated that further mutations will occur worldwide and probably even more after worldwide vaccination due to mutation force (Rahimi and Abadi 2021). Therefore, analyzing the effects of new strains of the SARS-CoV-2 virus is supremely significant. In the literature, a few authors proposed multi-variant mathematical models for COVID-19 (Gonzalez-Parra et al. 2021; Khyar and Allali 2020; Arruda et al. 2021). Gonzalez-Parra et al. (2021) studied the effect of a new, more infectious SARS-CoV-2 variant (VOC-202012/01 of lineage B.1.1.7) on hospitalizations, prevalence, and deaths associated with the SARS-CoV-2 virus. Khyar and Allali (2020) proposed a multi-strain SEIR model with general incident rate and studied the global dynamics of the model. The authors also discussed the quarantine strategy for controlling the disease spread and fit the model to the Moroccan clinical data of COVID-19. Arruda et al. (2021) proposed a model for COVID-19 and studied the optimal control of multi-strain epidemics.

Vaccination has been an effective strategy in battling the spread of contagious diseases, e.g., measles, influenza, and pertussis. In history, the elimination of smallpox has been counted as the most notable victory of vaccination ever recorded (World Health Organization 2021c). Several authors in multiple papers have investigated the role of vaccination (Cai et al. 2012; Castillo-Chavez et al. 2002; Scherer and McLean 2002; Liu et al. 2008; Arino et al. 2003; Gumel et al. 2006; Cai et al. 2018; Alexander et al. 2004). Under vaccination concern, certain mutant strains will finally have the competitive benefits amongst their contacts (Scherer and McLean 2002). Mathematical

models are helpful to describe and understand the dynamics of different strains under mutation and vaccination. The impact of vaccination on the growth of strain contacts in multi-strain viruses has been analyzed in many papers (Cai et al. 2012; Fudolig and Howard 2020; Gupta et al. 1997; Martcheva et al. 2007; May and Nowak 1994; McLean 1995; Porco and Blower 1998, 2000). Cai et al. (2012) proposed a two-strain model with vaccination. The authors studied the existence and stability of the equilibria as well as the existence of Hopf bifurcation from endemic equilibria. Martcheva et al. (2007) considered an epidemic model with vaccination and two competing strains. The authors engrossed on the ability of vaccination to generate subthreshold persistence of the disease and the consequences that this may occur when multiple strains are present. Porco and Blower (1998, 2000) analyzed mathematical models to assess the impact of vaccine programs to contain two variants of HIV and resulted different conditions for eradication of two variants in case of mass vaccination. McLean (1995) studied the different properties of the vaccine efficacy for the eradication of two different variants by developing a mathematical model. Gupta et al. (1997) analyzed that a vaccine consisting of the most immunogenic combinations of antigenic variants can cause a dramatic increase in frequency of a subset of rare strains. With the latest development of anti-COVID vaccines, a few models have been proposed to provide insight into the impact of vaccination of a certain fraction of the populace on the dynamics of the COVID-19 pandemic. For instance, Fudolig and Howard (2020) proposed a multi-strain model with vaccination for COVID-19 and studied the conditions for existence and local stability of equilibria. Furthermore, there is evidence of COVID-19 vaccine efficacy in Australia. The mRNA vaccine has shown over 90% efficacy against COVID-19 infection, the ChAdOx1 nCoV-19 vaccine has a 62% efficacy against symptomatic infection in the intended two-dose schedule, and the BNT162b2 mRNA vaccine has a 95% efficacy against symptomatic infection (MacIntyre et al. 2021). Also, the Pfizer-BioNTech BNT162b2 mRNA vaccine has an efficacy over 95%, Johnson & Johnson [J&J] Ad26 has an efficacy over 67%, the AstraZeneca-Oxford ChAdOx1 nCov-19 vaccine has an efficacy over 67%, and the Gamaleya GamCovidVac [Sputnik V] vaccine has the efficacy over 90% (Olliaro et al. 2021). According to the Ministry of Health and Family Welfare, Government of India, the Indian vaccine also has vaccine efficacy over 70–90% (Ministry of Health and Family Welfare 2021).

To determine effectual countermeasures, it is significant to develop mathematical models that support us in predicting and understanding the spread of COVID-19 and providing suitable control strategies. Mathematical modeling in epidemiology provides a progressively greater room to public health research. This research discipline participates to sufficiently comprehend the studied epidemiological phenomenon and capture the distinct issues that can give rise to a terrible epidemic or even an alarming pandemic worldwide. The classical susceptible-infected-recovered (SIR) epidemic model was first proposed by Kermack and McKendrick (1927). To obtain a sharper understanding of various vaccination strategies and their impacts on the number of infected individuals, Kermack-McKendrick type models have grabbed a vital role. This type of model has been benefited to comprehend vaccination dynamics on various diseases (Alexander et al. 2004). It is essential to emphasize that, Kermack-McKendrick kind mathematical models have helped in explaining COVID-19 epidemics properties worldwide. These models have been utilized to estimate the basic reproductive

number associated with the disease and various parameters engaged in its spread. Additional use of this type of models has been focused on proposing and assessing the impact of different control measures categorized as NPIs. For example, the authors in papers (Bugalia et al. 2020, 2021; Bajiya et al. 2020) proposed mathematical models for COVID-19 and analyzed the impact of NPIs on the disease dynamics. It is of paramount significance to develop mathematical models that can perfectly forecast the spread of COVID-19 so that the disease can be controlled and restrictions can be securely relaxed. However, the infection incubation period may occupy a long time interval in some cases. An incubated person is not yet infectious in this time interval and remains latent. Therefore another compartment of exposed individuals should be included in SIR, and the new model will termed as SEIR (Hethcote 2000).

Inspired by the evidence mentioned above about imperfect vaccine and mutation of the virus, in this work, we utilize an SEIR-type mathematical model to comprehend the dynamics of disease spread on the human populace under imperfect vaccination and two variants of the virus. The general methodology and mathematical model can be inferred to enhance the number of parameters and differential equations. We incorporate the vaccination compartment to the two-strain model to examine the effectiveness of the anti-COVID-19 vaccination, which is currently being employed in many countries to help battle the intense pandemic situation. It is supposed that the spread of a virus may mutate in the host to make a second, co-circulating, mutant strain. After some period of infection, the original strain, referred to as native strain, is converted to a mutant strain, such that a proportion of the people infected by the original strain are also carrying mutant strain. Thus we consider mutation in our proposed epidemic model. We intend to study the dynamical behavior of the strains' contacts under the vaccination scheme and investigate the impact of parameters (vaccination proportion, mutation rate, etc.) to demonstrate how they influence disease transmission. We also assume that recovered individuals from native strain have 100% immunity against native strain but may get infected by mutant strain. The objectives of the present study are the following: (i) construction of an epidemic model describing the dynamics of mutant strain under imperfect vaccination, (ii) investigation of the impact of an imperfect vaccine on the disease burden, (iii) investigation of different bifurcations with respect to significant parameters, (iv) application of the proposed model to the data of COVID-19 in India, (v) observation of the COVID-19 dynamics with respect to the key parameter related to the vaccine efficacy and mutation.

The remaining paper is organized as follows. Section 2 describes the proposed model with imperfect vaccine and mutation. Section 3 represents the dynamical analysis of the proposed system including the non-negativity and boundedness of solutions, basic reproduction number, existence, and stability of possible equilibria, transcritical bifurcation, and Hopf bifurcation. Section 4 describes the implications of disease control and explicit expression of vaccine-induced herd immunity. Numerical evaluations have been presented in Sect. 5. Cumulative cases and cumulative mortality data for COVID-19 pandemic in India have been used to parametrize the model, and the impact of different parameters on the cumulative cases and deaths have been shown in Sect. 6. Sensitivity analysis of the parameters with respect to the basic reproduction number, cumulative cases, and cumulative deaths has been performed in Sect. 7. The paper ends with a thorough discussion in Sect. 8.

2 Model formulation

We introduce a homogeneous two-strain model with imperfect vaccination. The system starts with a population exposed to both the native (original) and mutant (variant of original) strains of the virus. A few studies (Eletreby et al. 2020; Yagan et al. 2021) have revealed that SARS-CoV-2 mutates independently within the host, leading to infection with mutated strains that exhibit varying levels of transmissibility. Some previous studies (Gonzalez-Parra et al. 2021; Deng et al. 2021) exposed that the variant is more transmissible and severe than the original strain, and antibody neutralization is reduced in COVID-19 patients and vaccine recipients in various countries, including the US. Nature news (Nature news 2021) has reported that the mutant strain is spreading quickly in India and has become the dominant strain. A mutation is accounted for in epidemic models through a term that transfers individuals infected with one of the strains into individuals infected with the other (Bonhoeffer and Nowak 1994; Liu et al. 2018; Iwami et al. 2007; Cai et al. 2012; Martcheva 2015). We assume that vaccination is applied only to healthy individuals, therefore only susceptible individuals get vaccinated. Further, we also assume that the vaccine is imperfect, that is, the vaccinated individuals can become infected with both native and mutant strains of the virus. That happens at reduced transmission rates $\delta_1\beta_1$ and $\delta_2\beta_2$, where $0 \leq \delta_1 \leq 1, 0 \leq \delta_2 \leq 1$ are the reduction coefficients of native and mutant strains, respectively. If $\delta_1 = 0$, then vaccinated individuals will not get infected with native strain, i.e., the vaccine is perfect for native strain, and $\delta_1 = 1$ means vaccinated individuals get infected just like susceptible individuals, i.e., vaccine plays no protective role to native strain. Here $1 - \delta_1$ describes the vaccine efficacy against native strain. A similar scenario applies to the mutant strain, and $1 - \delta_2$ describes the vaccine efficacy against the mutant strain. Some vaccinated individuals can go back to susceptible individuals due to partial immunity. There are some shreds of evidence that there is a chance of a second COVID-19 infection after being diagnosed with first, from which recovered (Health, The Sciences 2021; Shastri et al. 2021; Centers for Disease Control and Prevention (CDC) 2021b). Therefore, we assume that the recovered individuals of native strain can also become infected via mutant strain of the virus at a reduced rate $\delta_3\beta_2$.

The model is composed of a system of differential equations that has eight compartments: susceptible compartment S—individuals in this compartment are healthy but can be infected by both the native and mutant strains of the virus; vaccinated compartment V—individuals that applied to vaccination, these individuals can also become infected by both the native and mutant strains of the virus but at lower rates; exposed compartment E_1—individuals that are exposed to a native strain of virus; exposed compartment E_2—individuals that are exposed to a mutant strain of virus; infected compartment I_1—individuals that are infected to a native strain of virus; infected compartment I_2—individuals that are infected to a mutant strain of virus; recovered compartment R_1—individuals that were infected to native strain, and are now immune to the native strain but not immune to the mutant strain; recovered compartment R_2—individuals that were infected to mutant strain are now immune to both native and mutant strains and do not interact with the remaining compartments. The biological interpretations of the parameters involved in the model are given in Table 1.

Table 1 Biological interpretations of parameters

Parameters	Biological interpretations
Λ	The recruitment rate at which new individuals enter in the susceptible population
β_1	Infection rate of the native strain
β_2	Infection rate of the mutant strain
p	Per capita vaccination rate of susceptible individuals
$1/\mu$	Average life expectancy of the individuals of all compartments
$1-\delta_1$	Efficacy of vaccine to native strain
$1-\delta_2$	Efficacy of vaccine to mutant strain
γ	Per capita rate of lost of immunity of vaccinated individuals
a_1	Per capita rate at which the exposed individuals of native strain become infectious
a_2	Per capita rate at which the exposed individuals of mutant strain become infectious
α_1	Per capita recovery rate of native strain
α_2	Per capita recovery rate of mutant strain
d_1	Per capita death rate due to native strain
d_2	Per capita death rate due to mutant strain
δ_3	Reduction coefficient of infection after recovery
ν_1	Per capita mutation rate of native strain

The schematic diagram of the model is given in Fig. 1. The total population size is $N(t) = S(t) + V(t) + E_1(t) + E_2(t) + I_1(t) + I_2(t) + R_1(t) + R_2(t)$.

Based on the parameters given in Table 1 and schematic diagram 1, the dynamics of the disease transmission can be governed by the following system of ordinary differential equations:

$$\begin{aligned}
\frac{dS}{dt} &= \Lambda - \beta_1 I_1 S - \beta_2 I_2 S - (\mu + p)S + \gamma V,\\
\frac{dV}{dt} &= pS - \delta_1\beta_1 I_1 V - \delta_2\beta_2 I_2 V - (\mu + \gamma)V,\\
\frac{dE_1}{dt} &= \beta_1(S + \delta_1 V)I_1 - (a_1 + \mu)E_1,\\
\frac{dE_2}{dt} &= \beta_2(S + \delta_2 V + \delta_3 R_1)I_2 - (a_2 + \mu)E_2,\\
\frac{dI_1}{dt} &= a_1 E_1 - (\alpha_1 + \mu + d_1 + \nu_1)I_1,\\
\frac{dI_2}{dt} &= a_2 E_2 - (\alpha_2 + \mu + d_2)I_2 + \nu_1 I_1,\\
\frac{dR_1}{dt} &= \alpha_1 I_1 - \delta_3\beta_2 I_2 R_1 - \mu R_1,\\
\frac{dR_2}{dt} &= \alpha_2 I_2 - \mu R_2,
\end{aligned} \tag{1}$$

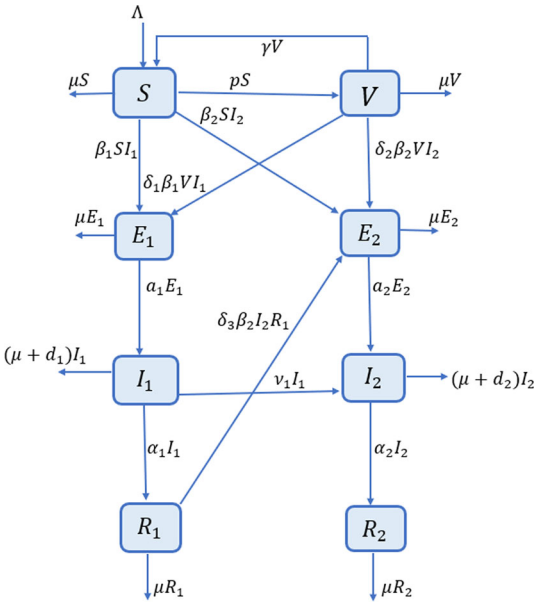

Fig. 1 Schematic diagram of system (1)

with the initial conditions: $S(0) > 0, V(0) \geq 0, E_1(0) \geq 0, E_2(0) \geq 0, I_1(0) \geq 0, I_2(0) \geq 0, R_1(0) \geq 0, R_2(0) \geq 0$.

3 Rigorous analysis

This section is devoted to investigating the dynamical behaviors of system (1) including positivity and boundedness of the solutions, computation of the basic reproduction number, the existence of possible equilibria and their stability, and possible bifurcations. Firstly, we prove the positivity and boundedness of the solutions of system (1). Positivity is significant for biologically feasible solutions of the system while boundedness infers that solutions are finite. System (1) is given by the following bounded planes:

$$\left.\frac{dS}{dt}\right|_{S=0,V\neq0,E_1\neq0,E_2\neq0,I_1\neq0,I_2\neq0,R_1\neq0,R_2\neq0} = \Lambda + \gamma V > 0,$$

$$\left.\frac{dV}{dt}\right|_{S\neq0,V=0,E_1\neq0,E_2\neq0,I_1\neq0,I_2\neq0,R_1\neq0,R_2\neq0} = pS \geq 0,$$

$$\left.\frac{dE_1}{dt}\right|_{S\neq0,V\neq0,E_1=0,E_2\neq0,I_1\neq0,I_2\neq0,R_1\neq0,R_2\neq0} = \beta_1(S + \delta_1 V)I_1 \geq 0,$$

$$\left.\frac{dE_2}{dt}\right|_{S\neq0,V\neq0,E_1\neq0,E_2=0,I_1\neq0,I_2\neq0,R_1\neq0,R_2\neq0} = \beta_2(S + \delta_2 V)I_2 + \delta_3\beta_2 I_2 R_1 \geq 0,$$

$$\left.\frac{dI_1}{dt}\right|_{S\neq 0,V\neq 0,E_1\neq 0,E_2\neq 0,I_1=0,I_2\neq 0,R_1\neq 0,R_2\neq 0} = a_1E_1 \geq 0,$$

$$\left.\frac{dI_2}{dt}\right|_{S\neq 0,V\neq 0,E_1\neq 0,E_2\neq 0,I_1\neq 0,I_2=0,R_1\neq 0,R_2\neq 0} = a_2E_2 + \nu_1 I_1 \geq 0,$$

$$\left.\frac{dR_1}{dt}\right|_{S\neq 0,V\neq 0,E_1\neq 0,E_2\neq 0,I_1\neq 0,I_2\neq 0,R_1=0,R_2\neq 0} = \alpha_1 I_1 \geq 0,$$

$$\left.\frac{dR_2}{dt}\right|_{S\neq 0,V\neq 0,E_1\neq 0,E_2\neq 0,I_1\neq 0,I_2\neq 0,R_1\neq 0,R_2=0} = \alpha_2 I_2 \geq 0.$$

Note that on each of the bounding planes of the non-negative cone of $\mathbb{R}^8_+$, all rates in the system (1) are non-negative. Thus, if we initiate in the interior of this cone, we shall always remain in this cone as the direction of the vector field is inward on all the bounding planes. Therefore, the non-negativity of all solutions is guaranteed if we start from a non-negative initial point. Furthermore, system (1) also states that the total population N follows the below differential equation:

$$\frac{dN}{dt} = \Lambda - \mu N - d_1 I_1 - d_2 I_2, \tag{2}$$

which gives

$$\Lambda - (\mu + d_1 + d_2)N \leq \frac{dN}{dt} \leq \Lambda - \mu N.$$

Now integrating the above inequality and using initial conditions, we obtain

$$\begin{aligned}&\frac{\Lambda}{\mu + d_1 + d_2} + \left(N(0) - \frac{\Lambda}{\mu + d_1 + d_2}\right)e^{-(\mu+d_1+d_2)t}\\ &\leq N(t) \leq \frac{\Lambda}{\mu} + \left(N(0) - \frac{\Lambda}{\mu}\right)e^{-\mu t},\end{aligned}$$

Considering $t \to +\infty$, we obtain

$$\frac{\Lambda}{\mu + d_1 + d_2} \leq \liminf_{t\to+\infty} N(t) \leq \limsup_{t\to+\infty} N(t) \leq \frac{\Lambda}{\mu},$$

which implies the feasible region for system (1) and hence the positively invariant set for system (1), denoted by Δ, is given by

$$\begin{aligned}\Delta = \Bigg\{&(S, V, E_1, E_2, I_1, I_2, R_1, R_2) \in \mathbb{R}^8_+ : \frac{\Lambda}{\mu + d_1 + d_2}\\ &\leq S + V + E_1 + E_2 + I_1 + I_2 + R_1 + R_2 \leq \frac{\Lambda}{\mu} \subset \mathbb{R}^8_+\Bigg\}.\end{aligned} \tag{3}$$

From the above analysis, we conclude the following consequence:

Theorem 3.1 *The dynamics of system* (1) *would attract to the positively invariant set* Δ.

Therefore, the system (1) is well-posed and epidemiologically feasible since all variables remain nonnegative for all $t \geq 0$. Further, since the right hand side functions of each equations of system (1) are continuous and have continuous partial derivatives, then they satisfy the Lipschitz condition. Additionally, from Theorem 3.1, system (1) is uniformly bounded. Hence, the solution of system (1) exists and is unique.

3.1 Disease free equilibrium (DFE) and basic reproduction number

The disease free equilibrium (DFE) can be obtained by setting all infected variables (E_1, E_2, I_1, I_2) equal to zero while all non-infected variables (S, V, R_1, R_2) are non-zero. The DFE of system (1) is given by

$$\begin{aligned} D^0 &= (S^0, V^0, E_1^0, E_2^0, I_1^0, I_2^0, R_1^0, R_2^0) \\ &= \left(\frac{\Lambda(\mu+\gamma)}{\mu(\mu+\gamma+p)}, \frac{\Lambda p}{\mu(\mu+\gamma+p)}, 0, 0, 0, 0, 0, 0 \right). \end{aligned} \tag{4}$$

To obtain the basic reproduction number, we use the next generation method (Diekmann et al. 2010; Van den Driessche and Watmough 2002). By considering $x = (E_1, E_2, I_1, I_2)^T$, we have

$$x' = f(x) - v(x),$$

where

$$f = \begin{pmatrix} \beta_1(S+\delta_1 V)I_1 \\ \beta_2(S+\delta_2 V)I_2 + \delta_3\beta_2 I_2 R_1 \\ 0 \\ 0 \end{pmatrix}, \quad v = \begin{pmatrix} (a_1+\mu)E_1 \\ (a_2+\mu)E_2 \\ (\alpha_1+\mu+d_1+\nu_1)I_1 - a_1 E_1 \\ (\alpha_2+\mu+d_2)I_2 - \nu_1 I_1 - a_2 E_2 \end{pmatrix}.$$

The Jacobian of $f(x)$ and $v(x)$ at D^0 are

$$F = Df(D^0) = \begin{pmatrix} 0 & 0 & \beta_1(S^0+\delta_1 V^0) & 0 \\ 0 & 0 & 0 & \beta_2(S^0+\delta_2 V^0) \\ 0 & 0 & 0 & 0 \\ 0 & 0 & 0 & 0 \end{pmatrix},$$

and

$$V = Dv(D^0) = \begin{pmatrix} (a_1+\mu) & 0 & 0 & 0 \\ 0 & (a_2+\mu) & 0 & 0 \\ -a_1 & 0 & (\alpha_1+\mu+d_1+\nu_1) & 0 \\ 0 & -a_2 & -\nu_1 & (\alpha_2+\mu+d_2) \end{pmatrix},$$

respectively. The next generation matrix FV^{-1} is given by

$$FV^{-1} = \begin{pmatrix} \frac{\beta_1 a_1(S^0+\delta_1 V^0)}{(a_1+\mu)(\alpha_1+d_1+\mu+\nu_1)} & 0 & \frac{\beta_1(S^0+\delta_1 V^0)}{\alpha_1+d_1+\mu+\nu_1} & 0 \\ \frac{a_1\beta_2\nu_1(S^0+\delta_2 V^0)}{(a_1+\mu)(\alpha_2+d_2+\mu)(\alpha_1+d_1+\mu+\nu_1)} & \frac{\beta_2 a_2(S^0+\delta_2 V^0)}{(a_2+\mu)(\alpha_2+d_2+\mu)} & \frac{\beta_2\nu_1(S^0+\delta_2 V^0)}{(\alpha_2+d_2+\mu)(\alpha_1+d_1+\mu+\nu_1)} & \frac{\beta_2(S^0+\delta_2 V^0)}{\alpha_2+d_2+\mu} \\ 0 & 0 & 0 & 0 \\ 0 & 0 & 0 & 0 \end{pmatrix}.$$

Hence, the basic reproduction number for system (1) is the dominant eigenvalue or spectral radius of the next generation matrix FV^{-1}, which implies

$$R_0 = \rho(FV^{-1}) = \max\{R_1, R_2\}, \tag{5}$$

where

$$R_1 = \frac{\beta_1 a_1(S^0+\delta_1 V^0)}{(\mu+a_1)(\mu+d_1+\alpha_1+\nu_1)} = \frac{\Lambda\beta_1 a_1(\gamma+\mu+p\delta_1)}{\mu(\mu+a_1)(\mu+d_1+\alpha_1+\nu_1)(p+\gamma+\mu)},$$
$$R_2 = \frac{\beta_2 a_2(S^0+\delta_2 V^0)}{(\mu+a_2)(\mu+d_2+\alpha_2)} = \frac{\Lambda\beta_2 a_2(\gamma+\mu+p\delta_2)}{\mu(\mu+a_2)(\mu+d_2+\alpha_2)(p+\gamma+\mu)}.$$

Here $R_1(R_2)$ represents the average number of secondary infection cases generated by a single infectious individual of the native (mutant) strain of the virus, called the basic reproduction number of the native (mutant) strain.

3.1.1 Interpretation of the basic reproduction number

As stated above, the basic reproduction number R_0 is the maximum of the two basic reproduction numbers, R_1 and R_2. The basic reproduction number R_1 is given by the product of the infection rate of the susceptible (unvaccinated) and vaccinated individuals by native strain infectious individuals (near the disease-free equilibrium) $[\beta_1(S^0+\delta_1 V^0)]$, the proportion of the exposed individuals to the native strain that survived in the exposed class (E_1) and moved to infected compartment (I_1) $[\frac{a_1}{\mu+a_1}]$, and the average time duration in the infectious class (I_1) $[\frac{1}{\mu+d_1+\alpha_1+\nu_1}]$. Similarly, the basic reproduction number R_2 is given by the product of the infection rate of the susceptible (unvaccinated) and vaccinated individuals by the mutant strain infectious individuals (near the disease-free equilibrium), $[\beta_2(S^0+\delta_1 V^0)]$, the proportion of the exposed individuals to the mutant strain that survived in the exposed class (E_2) and moved to infected compartment (I_2) $[\frac{a_2}{\mu+a_2}]$, and the average time duration in the infectious class (I_2) $[\frac{1}{\mu+d_2+\alpha_2}]$.

Remark 3.2 If $\delta_1 = 0, \delta_2 = 0$, then vaccine is perfectly effective to both native and mutant strains and if $p = 0$ then the system reduces without vaccination. For this case, the basic reproduction numbers of the native strain and mutant strain, R_{1wv} and R_{2wv} are given by, respectively,

$$R_{1wv} = \frac{\Lambda\beta_1 a_1}{\mu(\mu+a_1)(\mu+d_1+\alpha_1+\nu_1)},$$

$$R_{2wv} = \frac{\Lambda\beta_2 a_2}{\mu(\mu + a_2)(\mu + d_2 + \alpha_2)}.$$

Thus, the basic reproduction number of system without vaccination is given by $R_{0wv} = \max\{R_{1wv}, R_{2wv}\}$.

Theorem 3.3 *1. D^0 is locally asymptotically stable, whenever $R_0 = \max\{R_1, R_2\} < 1$; otherwise unstable.*
2. D^0 is globally asymptotically stable, whenever $R_0 = \max\{R_1, R_2\} < 1$.

Proof 1. We first prove the local asymptotic stability of D^0. By linearizing the system (1) at D^0, we obtain the following characteristic equation

$$\begin{aligned}&(\lambda+\mu)^3(\lambda+p+\gamma+\mu)(\lambda^2+\lambda(2\mu+a_1+d_1+\alpha_1)\\&\quad+(\mu+a_1)(\mu+d_1+\alpha_1+\nu_1)(1-R_1))\\&(\lambda^2+\lambda(2\mu+a_2+d_2+\alpha_2)+(\mu+a_2)(\mu+d_2+\alpha_2)(1-R_2))=0.\end{aligned} \tag{6}$$

From the above characteristic equation, it is easy to observe that all the roots of Eq. (6) are negative or have negative real parts for $R_0 < 1$. Hence, the D^0 of system (1) is locally asymptotically stable for $R_0 < 1$. If $R_0 > 1$, at least one of the roots of Eq. (6) has positive real part. Hence, D^0 is unstable for $R_0 > 1$.
2. To prove the global stability of D^0, we follow the approach given by Castillo-Chavez et al. (2002). We rewrite the system (1) as follows

$$\begin{aligned}\frac{dX}{dt} &= F(X, Y),\\ \frac{dY}{dt} &= G(X, Y), \quad G(X, 0) = 0,\end{aligned} \tag{7}$$

where $X = (S, V, R_1, R_2) \in \mathbb{R}^4$ signifies the number of uninfected individuals and $Y = (E_1, E_2, I_1, I_2) \in \mathbb{R}^4$ signifies the number of infected individuals. Disease-free equilibrium (D^0) is globally stable if the following two conditions are fulfilled:

(H1) For $\frac{dX}{dt} = F(X, Y)$, X^* is globally asymptotically stable,
(H2) $G(X, Y) = MY - \hat{G}(X, Y)$, $\hat{G}(X, Y) > 0$ for $(X, Y) \in \Delta$,

where $M = D_Y G(X^*, 0)$ is an M-matrix. For the system (1), we have

$$F(X, 0) = \begin{pmatrix} \Lambda - (\mu + p)S + \gamma V \\ pS - (\mu + \gamma)V \\ 0 \\ 0 \end{pmatrix}. \tag{8}$$

It is obvious that the equilibrium $X^* = \left(\frac{\Lambda(\mu+\gamma)}{\mu(\mu+\gamma+p)}, \frac{\Lambda p}{\mu(\mu+\gamma+p)}, 0, 0\right)$ of system (8) is globally asymptotically stable. Further for system (1), we obtain

$$M = \begin{pmatrix} -(\mu+a_1) & 0 & \beta_1(S^0+\delta_1 V^0) & 0 \\ 0 & -(\mu+a_2) & 0 & \beta_2(S^0+\delta_2 V^0) \\ a_1 & 0 & -(\alpha_1+\mu+d_1+\nu_1) & 0 \\ 0 & a_2 & \nu_1 & -(\alpha_2+\mu+d_2) \end{pmatrix},$$

$$\hat{G}(X,Y) = \begin{pmatrix} \beta_1 I_1((S^0+\delta_1 V^0)-(S+\delta_1 V)) \\ \beta_2 I_2((S^0+\delta_2 V^0)-(S+\delta_2 V+\delta_3 R_1)) \\ 0 \\ 0 \end{pmatrix}.$$

It is clear that $\hat{G}(X,Y) \geq 0$. Hence, D^0 is globally stable, i.e. every solution of the system (1) approaches the DFE (D^0) as $t \to \infty$ for $R_0 < 1$. Thus, the disease (i.e., both native and mutant strains) will be eliminated from the community if $R_0 < 1$. Consequently, R_0 represents the threshold value for the existence of other positive equilibria of the system (1). Moreover, it is well known that the basic reproduction number (R_0) represents the average number of secondary infections that occurred from a single infectious individual in the whole susceptible population in its entire infectious period. Therefore, if $R_0 < 1$, each infectious individual in the entire infectious period will produce less than one infected individual on average, which implies that the disease will die out. However, if $R_0 > 1$, then each infectious individual in the whole infectious period having contact with susceptible individuals will generate more than one infected individual; this leads to the disease invading the susceptible population. □

It must be mentioned that for mathematical (endemic) models such as (1), the epidemiological necessity $R_0 < 1$ is sufficient as well as necessary for eradication of the disease. This is because, for such mathematical models (i.e., Kermack-McKendrick models with demographic dynamics), the disease will persist whenever $R_0 > 1$ (this is because the pool of new susceptible individuals will continuously be refilled, by immigration or birth, thereby letting the disease to maintain itself in the community). If the demographic effects are not allowed (i.e., in the case of a single outbreak/epidemic model is used), the epidemiological condition $R_0 < 1$ is only sufficient but not necessary for eradicating the epidemic. For such epidemic models (with no demographic dynamics), the disease always dies out with time (irrespective of the value of the basic reproduction number of the epidemic models). In other words, even if the basic reproduction number exceeds unity, the disease will eventually die out; this is because the epidemic rises and reaches a peak.

3.2 Mutant dominant equilibrium and its stability

First of all, it should be mentioned that in the absence of native strain ($I_1 = 0$), the system (1) reduces to the following subsystem:

$$\begin{aligned}
\frac{dS}{dt} &= \Lambda - \beta_2 I_2 S - (\mu + p)S + \gamma V,\\
\frac{dV}{dt} &= pS - \delta_2\beta_2 I_2 V - (\mu + \gamma)V,\\
\frac{dE_2}{dt} &= \beta_2(S + \delta_2 V)I_2 - (a_2 + \mu)E_2,\\
\frac{dI_2}{dt} &= a_2 E_2 - (\alpha_2 + \mu + d_2)I_2,\\
\frac{dR_2}{dt} &= \alpha_2 I_2 - \mu R_2.
\end{aligned} \tag{9}$$

The analysis of the sub-system (9) will be considered in the following positively invariant region

$$\Delta_{I_2} = \left\{(S, V, E_2, I_2, R_2) \in \mathbb{R}^5_+ : 0 < S + V + E_2 + I_2 + R_2 \leq \frac{\Lambda}{\mu} \subset \mathbb{R}^5_+\right\}.$$

The mutant dominant (boundary) equilibrium is given by $D^2 = (S^2, V^2, 0, E_2^2, 0, I_2^2, 0, R_2^2)$, where the components of D^2 can be obtained by solving the equations of right hand side of the subsystem (9). Thus,

$$\begin{aligned}
S^2 &= \frac{\Lambda}{\mu} - \frac{p\left\{\Lambda a_2 - (a_2 + \mu)(\alpha_2 + \mu + d_2)I_2^2\right\}}{\mu a_2(\delta_2\beta_2 I_2^2 + \mu + \gamma + p)} - \frac{(a_2 + \mu)(\alpha_2 + \mu + d_2)I_2^2}{\mu a_2},\\
V^2 &= \frac{p\left\{\Lambda a_2 - (a_2 + \mu)(\alpha_2 + \mu + d_2)I_2^2\right\}}{\mu a_2(\delta_2\beta_2 I_2^2 + \mu + \gamma + p)}, \quad E_2^2 = \frac{(\alpha_2 + \mu + d_2)I_2^2}{a_2}, \quad R_2^2 = \frac{\alpha_2 I_2^2}{\mu},
\end{aligned}$$

and I_2^2 satisfies the following equation:

$$k_1' I_2^2 + k_2' I_2 + k_3' = 0, \tag{10}$$

where

$$\begin{aligned}
k_1' &= \beta_2^2(\mu + a_2)(\mu + d_2 + \alpha_2)\delta_2,\\
k_2' &= \beta_2((\mu + a_2)(\mu + d_2 + \alpha_2)(\gamma + \mu + (p + \mu)\delta_2) - \Lambda\beta_2 a_2\delta_2),\\
k_3' &= \mu(\mu + a_2)(\mu + d_2 + \alpha_2)(\gamma + \mu + p)(1 - R_2).
\end{aligned}$$

We can see that Eq. (10) has zero, one, or two roots, depending on parameter values. For the case $0 < \delta_2 \leq 1$, $k_3' < 0$ if $R_2 > 1$, and $k_3' > 0$ if $R_2 < 1$. Since Eq. (10) is a quadratic equation, therefore if $R_2 > 1$, then Eq. (10) has a unique positive root and there is a unique mutant dominant equilibrium. If $R_2 = 1$, then $k_3' = 0$ and there is unique non-zero solution of (10), given by $I_2^2 = -\frac{k_2'}{k_1'}$, which is positive if and only if $k_2' < 0$. If $R_2 = 1, k_3' = 0$, then

$$\Lambda\beta_2 a_2(\gamma+\mu+p\delta_2)=\mu(\mu+a_2)(\mu+d_2+\alpha_2)(p+\gamma+\mu). \tag{11}$$

The condition $k_2^{'}<0$ gives

$$(\mu+a_2)(\mu+d_2+\alpha_2)(\gamma+\mu+(p+\mu)\delta_2)<\Lambda\beta_2 a_2\delta_2,$$

combined with (11), we obtain

$$(\gamma+\mu)^2+(p\delta_2)^2+\mu p\delta_2^2+2\gamma p\delta_2+\mu p\delta_2<0,$$

which is not possible. Hence, if $R_2\leq 1$, system (1) has no mutant dominant equilibrium. Furthermore, it should be stated that for the equilibrium D^2 to exist, it is necessary that the native strain dies out asymptotically (i.e., $R_1\leq 1$). Thus, we conclude that system (9) has a unique mutant dominant equilibrium (D^2) whenever $R_2>1$ and $R_1\leq 1$. Further, for the stability of the equilibrium D^2, we have the following result:

Theorem 3.4 *The unique mutant dominant equilibrium (D^2) is globally asymptotically stable whenever it exists.*

Proof We consider

$$x=\frac{S}{S^2},\ y=\frac{V}{V^2},\ z=\frac{E_2}{E_2^2},\ u=\frac{I_2}{I_2^2},$$

and with the help of right hand side of the system (9), the system (9) can be rewritten as follows:

$$\begin{aligned}
x' &= x\Big[\frac{\Lambda}{S^2}\Big(\frac{1}{x}-1\Big)-\beta_2 I_2^2(u-1)+\frac{\gamma V^2}{S^2}\Big(\frac{y}{x}-1\Big)\Big],\\
y' &= y\Big[\frac{pS^2}{V^2}\Big(\frac{x}{y}-1\Big)-\delta_2\beta_2 I_2^2(u-1)\Big],\\
z' &= z\frac{\beta_2 I_2^2}{E_2^2}\Big[S^2\Big(\frac{xu}{z}-1\Big)+\delta_2 V^2\Big(\frac{yu}{z}-1\Big)\Big],\\
u' &= u\frac{a_2 E_2^2}{I_2^2}\Big[\frac{z}{u}-1\Big].
\end{aligned} \tag{12}$$

Further, we consider the following Lyapunov function

$$\begin{aligned}
Z = \ & k_1 S^2(x-1-\ln x)+k_2 V^2(y-1-\ln y)+k_3 E_2^2(z-1-\ln z)\\
&+k_4 I_2^2(u-1-\ln u),
\end{aligned}$$

where the positive constants k_1, k_2, k_3, and k_4 will be defined below. By differentiating Z with respect to t along the solutions of (9), we obtain

$$
\begin{aligned}
Z' &= k_1(x-1)\Big[\Lambda\Big(\frac{1}{x}-1\Big)-\beta_2 S^2 I_2^2(u-1)+\gamma V^2\Big(\frac{y}{x}-1\Big)\Big]\\
&\quad + k_2(y-1)\Big[ps^2\Big(\frac{x}{y}-1\Big)-\delta_2\beta_2 V^2 I_2^2(u-1)\Big]\\
&\quad + k_3\beta_2 I_2^2(z-1)\Big[S^2\Big(\frac{xu}{z}-1\Big)+\delta_2 V^2\Big(\frac{yu}{z}-1\Big)\Big]+k_4 a_2 E_2^2(u-1)\Big(\frac{z}{u}-1\Big)\\
&= k_1(2\Lambda+\gamma V^2-\beta_2 S^2 I_2^2)+k_2(pS^2-\delta_2\beta_2 V^2 I_2^2)+k_3(\beta_2 S^2 I_2^2+\delta_2\beta_2 V^2 I_2^2)\\
&\quad + k_4 a_2 E_2^2-(k_1\Lambda+k_1\gamma V^2-k_1\beta_2 S^2 I_2^2-k_2 pS^2)x-k_1\Lambda\frac{1}{x}\\
&\quad -(-k_1\gamma V^2+k_2 pS^2-k_2\delta_2\beta_2 V^2 I_2^2)y-k_1\gamma V^2\frac{y}{x}-k_2 pS^2\frac{x}{y}\\
&\quad -(k_1\beta_2 S^2 I_2^2-k_3\beta_2 S^2 I_2^2)ux-(-k_1\beta_2 S^2 I_2^2-k_2\delta_2\beta_2 V^2 I_2^2+k_4 a_2 E_2^2)u\\
&\quad -(k_2\delta_2\beta_2 V^2 I_2^2-k_3\delta_2\beta_2 V^2 I_2^2)yu-(k_3\beta_2 S^2 I_2^2+k_3\delta_2\beta_2 V^2 I_2^2-k_4 a_2 E_2^2)z\\
&\quad -k_3\beta_2 S^2 I_2^2\frac{xu}{z}-k_3\delta_2\beta_2 V^2 I_2^2\frac{yu}{z}-k_4 a_2 E_2^2\frac{z}{u}\\
&=: G(x,y,z,u).
\end{aligned}
$$

Choose the positive constants $k_1, k_2, k_3,$ and k_4 as follows:

$$k_1 = k_2 = k_3 = 1, k_4 = \frac{a_2+\mu}{a_2}.$$

Substituting the above values in the function $G(x, y, z, u)$, we obtain

$$
\begin{aligned}
G(x,y,z,u) &= 2\Lambda+\gamma V^2+pS^2+(a_2+\mu)E_2^2-\mu S^2 x-\Lambda\frac{1}{x}-\mu V^2 y-\gamma V^2\frac{y}{x}\\
&\quad - pS^2\frac{x}{y}-\beta_2 S^2 I_2^2\frac{xu}{z}-\delta_2\beta_2 V^2 I_2^2\frac{yu}{z}-(a_2+\mu)E_2^2\frac{z}{u}\\
&= \mu S^2\Big(2-x-\frac{1}{x}\Big)+\gamma V^2\Big(2-\frac{x}{y}-\frac{y}{x}\Big)+\mu V^2\Big(3-\frac{1}{x}-y-\frac{x}{y}\Big)\\
&\quad + \beta_2 S^2 I_2^2\Big(3-\frac{1}{x}-\frac{xu}{z}-\frac{z}{u}\Big)+\delta_2\beta_2 V^2 I_2^2\Big(4-\frac{1}{x}-\frac{x}{y}-\frac{yu}{z}-\frac{z}{u}\Big).
\end{aligned}
$$

By the property that the arithmetic mean is greater than or equal to the geometric mean, $G(x, y, z, u) \le 0$, and the equality holds only for $x = y = 1$ and $z = u$, i.e.,

$$
\begin{aligned}
&\big\{(x,y,z,u)\in\Delta_{I_2} : G(x,y,z,u)=0\big\}\\
&\quad\equiv\{(x,y,z,u) : x=y=1, z=u\},
\end{aligned}
$$

which corresponds to the set

$$\Delta'_{I_2}=\left\{(S,V,E_2,I_2) : S=S^*, V=V^*, \frac{E_2}{E_2^*}=\frac{I_2}{I_2^*}\right\}\subset\Delta_{I_2}\subset\Delta.$$

It is evident to see that the maximum invariant set of (9) on the set Δ'_{I_2} is the singleton $\{D^2\}$, therefore the mutant dominant equilibrium D^2 is globally stable in $\Delta_{I_2} \subset \Delta$ by LaSalle's Invariance Principle (LaSalle 1976). □

3.3 Coexistence equilibrium and its stability

This section examines the existence and global stability of the coexistence equilibrium of system (1). First of all, let us consider the endemic equilibrium $D^* = (S^*, V^*, E_1^*, E_2^*, I_1^*, I_2^*, R_1^*, R_2^*)$, then $S^*, V^*, E_1^*, E_2^*, I_1^*, I_2^*, R_1^*$, and R_2^* satisfy the following equations:

$$\begin{aligned}
&\Lambda - \beta_1 I_1 S - \beta_2 I_2 S - (\mu + p)S + \gamma V = 0,\\
&pS - \delta_1\beta_1 I_1 V - \delta_2\beta_2 I_2 V - (\mu + \gamma)V = 0,\\
&\beta_1(S + \delta_1 V)I_1 - (a_1 + \mu)E_1 = 0,\\
&\beta_2(S + \delta_2 V + \delta_3 R_1)I_2 - (a_2 + \mu)E_2 = 0,\\
&a_1 E_1 - (\alpha_1 + \mu + d_1 + \nu_1)I_1 = 0,\\
&a_2 E_2 - (\alpha_2 + \mu + d_2)I_2 + \nu_1 I_1 = 0,\\
&\alpha_1 I_1 - \delta_3\beta_2 I_2 R_1 - \mu R_1 = 0,\\
&\alpha_2 I_2 - \mu R_2 = 0.
\end{aligned} \tag{13}$$

The above Eqs. (13) lead the following expressions:

$$\begin{aligned}
S^* &= \frac{\Lambda(\beta_1\delta_1 I_1^* + \beta_2\delta_2 I_2^* + \mu + \gamma)}{(\beta_1 I_1^* + \beta_2 I_2^* + \mu + p)(\beta_1\delta_1 I_1^* + \beta_2\delta_2 I_2^* + \mu + \gamma) - p\gamma},\\
V^* &= \frac{\Lambda p}{(\beta_1 I_1^* + \beta_2 I_2^* + \mu + p)(\beta_1\delta_1 I_1^* + \beta_2\delta_2 I_2^* + \mu + \gamma) - p\gamma},\\
E_1^* &= \frac{(\alpha_1 + \mu + d_1 + \nu_1)I_1^*}{a_1}, \quad E_2^* = \frac{(\alpha_2 + \mu + d_2)I_2^* - \nu_1 I_1^*}{a_2},\\
R_1^* &= \frac{\alpha_1 I_1^*}{\delta_2\beta_2 I_2^* + \mu}, \quad R_2^* = \frac{\alpha_2 I_2^*}{\mu},
\end{aligned}$$

and I_1^*, I_2^* are the solutions of the following equations:

$$\begin{aligned}
F(I_1, I_2) \equiv &\beta_2^2\delta_2 I_2^2 + \beta_2\Big(-\frac{\Lambda\beta_1 a_1\delta_2}{(\mu + a_1)(\mu + d_1 + \alpha_1 + \nu_1)}\\
&+ \gamma + \mu + (p + \mu)\delta_2 + \beta_1(\delta_1 + \delta_2)I_1\Big)I_2\\
&+ \beta_1^2\delta_1 I_1^2 + \beta_1\Big(-\frac{\Lambda\beta_1 a_1\delta_1}{(\mu + a_1)(\mu + d_1 + \alpha_1 + \nu_1)} + \gamma + \mu + (p + \mu)\delta_1\Big)I_1\\
&+ \mu(p + \mu + \gamma)(1 - R_1) = 0,\\
G(I_1, I_2) \equiv &I_2^3\Big(\beta_2^2\delta_2\Big(1 - \frac{\Lambda a_2\beta_2\delta_2}{(\mu + a_2)(\mu + d_2 + \alpha_2)} - \frac{a_2\alpha_1\beta_2\delta_3 I_1}{(\mu + a_2)(\mu + d_2 + \alpha_2)}\Big)\Big)
\end{aligned}$$

$$
\begin{aligned}
&+ I_2^2\Bigg(\beta_2(\gamma+\mu+\delta_2(p+\mu)) \\
&- \frac{a_2\beta_2^2\delta_2\Lambda(\gamma+2\mu-p\delta_2)}{(\mu+a_2)(\mu+d_2+\alpha_2)} - \frac{I_1^2 a_2\alpha_1\beta_1\beta_2^2\delta_3(\delta_1+\delta_2)}{(\mu+a_2)(\mu+d_2+\alpha_2)} \\
&+ I_1\Big(\beta_1\beta_2(\delta_1+\delta_2) \\
&- \frac{\beta_2^2(a_2\alpha_1\delta_3(\gamma+\mu+(p+\mu)\delta_2)+\Lambda a_2\beta_1\delta_1\delta_2+(\mu+a_2)\delta_1\nu_1)}{(\mu+a_2)(\mu+d_2+\alpha_2)}\Big)\Bigg) \\
&+ I_2\Bigg(\mu(p+\gamma+\mu) - \frac{\Lambda\beta_2 a_2\mu(\gamma+\mu+p\delta_2)}{(\mu+a_2)(\mu+d_2+\alpha_2)} - \frac{a_2\alpha_1\beta_1^2\beta_2\delta_1\delta_3 I_1^3}{(\mu+a_2)(\mu+d_2+\alpha_2)} \\
&+ I_1^2\Big(1 - \frac{\beta_1\beta_2\delta_3\alpha_1 a_2(\gamma+\mu+(p+\mu)\delta_1)}{(\mu+a_2)(\mu+d_2+\alpha_2)} + \frac{(\delta_1+\delta_2)\nu_1}{(\mu+d_2+\alpha_2)}\Big) \\
&+ I_1\Big(\frac{\nu_1(\gamma+\mu+(p+\mu)\delta_2) - \beta_2\mu a_2\alpha_1\delta_3(\gamma+\mu+p) - \Lambda\mu a_2\beta_1\beta_2\delta_1}{(\mu+a_2)(\mu+d_2+\alpha_2)} \\
&+ \beta_1(\gamma+\mu+(p+\mu)\delta_1)\Big)\Bigg) - \frac{I_1}{(\mu+d_2+\alpha_2)}\Bigg(\nu_1\mu(p+\gamma+\mu) \\
&+ I_1\beta_1\nu_1(\gamma+\mu+(p+\mu)\delta_1) + I_1^2\beta_1^2\delta_1\nu_1\Bigg) = 0. \qquad (14)
\end{aligned}
$$

If the system (14) admits a solution, then the system (1) will have an endemic equilibrium. Obtaining the explicit expression for the exact solution of the non-linear autonomous system (14) is a daunting task. However, we will later show that the system (1) is uniformly persistent when $R_1 > 1$ and $R_2 > 1$, which implies that the system (1) has at least one endemic equilibrium. Here, we prove the global stability of the endemic equilibrium for a special case ($\delta_3 = 0$ and $\nu_1 = 0$) of system (1) in the subsequent theorem:

Theorem 3.5 *If the endemic equilibrium* $D^* = (S^*, V^*, E_1^*, E_2^*, I_1^*, I_2^*, R_1^*, R_2^*)$ *exists for* $\delta_3 = 0$ *and* $\nu_1 = 0$, *then it is globally asymptotically stable.*

Proof For $\delta_3 = 0$ and $\nu_1 = 0$, the endemic equilibrium $D^* = (S^*, V^*, E_1^*, E_2^*, I_1^*, I_2^*)$, S^*, V^*, E_1^*, E_2^*, I_1^*, and I_2^* satisfy the following equations:

$$
\begin{aligned}
&\Lambda - \beta_1 I_1 S - \beta_2 I_2 S - (\mu+p)S + \gamma V = 0, \\
&pS - \delta_1\beta_1 I_1 V - \delta_2\beta_2 I_2 V - (\mu+\gamma)V = 0, \\
&\beta_1(S+\delta_1 V)I_1 - (a_1+\mu)E_1 = 0, \\
&\beta_2(S+\delta_2 V)I_2 - (a_2+\mu)E_2 = 0, \\
&a_1 E_1 - (\alpha_1+\mu+d_1)I_1 = 0, \\
&a_2 E_2 - (\alpha_2+\mu+d_2)I_2 = 0.
\end{aligned} \qquad (15)
$$

Since R_1 and R_2 do not appear explicitly in the first six equations of system (1), therefore we omit them. By using the Eqs. (15) and denoting

$$x = \frac{S}{S^*},\ y = \frac{V}{V^*},\ z = \frac{E_1}{E_1^*},\ u = \frac{E_2}{E_2^*},\ v = \frac{I_1}{I_1^*},\ w = \frac{I_2}{I_2^*},$$

the system (1) can be rewritten as:

$$\begin{aligned}
x' &= x\Big[\frac{\Lambda}{S^*}\Big(\frac{1}{x}-1\Big) - \beta_1 I_1^*(v-1) - \beta_2 I_2^*(w-1) + \frac{\gamma V^*}{S^*}\Big(\frac{y}{x}-1\Big)\Big],\\
y' &= y\Big[\frac{pS^*}{V^*}\Big(\frac{x}{y}-1\Big) - \delta_1\beta_1 I_1^*(v-1) - \delta_2\beta_2 I_2^*(w-1)\Big],\\
z' &= z\frac{\beta_1 I_1^*}{E_1^*}\Big[S^*\Big(\frac{xv}{z}-1\Big) + \delta_1 V^*\Big(\frac{yv}{z}-1\Big)\Big],\\
u' &= u\frac{\beta_2 I_2^*}{E_2^*}\Big[S^*\Big(\frac{xw}{u}-1\Big) + \delta_2 V^*\Big(\frac{yw}{u}-1\Big)\Big],\\
v' &= v\frac{a_1 E_1^*}{I_1^*}\Big[\frac{z}{v}-1\Big],\\
w' &= w\frac{a_2 E_2^*}{I_2^*}\Big[\frac{u}{w}-1\Big].
\end{aligned} \tag{16}$$

It is clear that the endemic equilibrium D^* of (1) corresponds to the positive equilibrium $\bar{D}^*(1,1,1,1,1,1)$ of (16), and that the global stability of $\bar{D}^*$ is same as that of D^*, therefore, we will discuss the global stability of the equilibrium $\bar{D}^*$ of system (16) instead of D^*.

Define the Lyapunov function

$$\begin{aligned}
L = {} & k_1 S^*(x - 1 - \ln x) + k_2 V^*(y - 1 - \ln y) + k_3 E_1^*(z - 1 - \ln z)\\
& + k_4 E_2^*(u - 1 - \ln u) + k_5 I_1^*(v - 1 - \ln v) + k_6 I_2^*(w - 1 - \ln w),
\end{aligned}$$

where the positive numbers k_1, k_2, k_3, k_4, k_5, and k_6 will be given below, then differentiating L with respect to t along solutions of (16), we obtain

$$\begin{aligned}
L' = {} & k_1(x-1)\Big[\Lambda\Big(\frac{1}{x}-1\Big) - \beta_1 I_1^* S^*(v-1) - \beta_2 I_2^* S^*(w-1) + \gamma V^*\Big(\frac{y}{x}-1\Big)\Big]\\
& + k_2(y-1)\Big[pS^*\Big(\frac{x}{y}-1\Big) - \delta_1\beta_1 I_1^* V^*(v-1) - \delta_2\beta_2 I_2^* V^*(w-1)\Big]\\
& + k_3(z-1)\beta_1 I_1^*\Big[S^*\Big(\frac{xv}{z}-1\Big) + \delta_1 V^*\Big(\frac{yv}{z}-1\Big)\Big]\\
& + k_4(u-1)\beta_2 I_2^*\Big[S^*\Big(\frac{xw}{u}-1\Big) + \delta_2 V^*\Big(\frac{yw}{u}-1\Big)\Big]\\
& + k_5(v-1)a_1 E_1^*\Big[\frac{z}{v}-1\Big] + k_6(w-1)a_2 E_2^*\Big[\frac{u}{w}-1\Big]\\
= {} & k_1(2\Lambda - \beta_1 S^* I_1^* - \beta_2 S^* I_2^* + \gamma V^*) + k_2(pS^* - \delta_1\beta_1 V^* I_1^* - \delta_2\beta_2 V^* I_2^*)\\
& + k_3(\beta_1 S^* I_1^* + \delta_1\beta_1 V^* I_1^*) + k_4(\beta_2 S^* I_2^* + \delta_2\beta_2 V^* I_2^*) + k_5 a_1 E_1^* + k_6 a_2 E_2^*\\
& - (k_1\Lambda - k_1\beta_1 S^* I_1^* - k_1\beta_2 S^* I_2^* + k_1\gamma V^* - k_2 pS^*)x - k_1\Lambda\frac{1}{x}
\end{aligned}$$

$$
\begin{aligned}
&- (-k_1\gamma V^* + k_2 pS^* - k_2\delta_1\beta_1 V^* I_1^* - k_2\delta_2\beta_2 V^* I_2^*)y \\
&- (k_1\beta_1 S^* I_1^* - k_3\beta_1 S^* I_1^*)xv - (-k_1\beta_1 S^* I_1^* - k_2\delta_1\beta_1 V^* I_1^* + k_5 a_1 E_1^*)v \\
&- (k_1\beta_2 S^* I_2^* - k_4\beta_2 S^* I_2^*)xw \\
&- (-k_1\beta_2 S^* I_2^* - k_2\delta_2\beta_2 V^* I_2^* + k_6 a_2 E_2^*)w - k_1\gamma V^* \frac{y}{x} \\
&- k_2 pS^* \frac{x}{y} - k_3\beta_1 S^* I_1^* \frac{xv}{z} \\
&- k_3\beta_1\delta_1 V^* I_1^* \frac{yv}{z} - k_4\beta_2 S^* I_2^* \frac{xw}{u} - k_4\beta_2\delta_2 V^* I_2^* \frac{yw}{u} \\
&- (k_1\delta_1\beta_1 V^* I_1^* - k_3\delta_1\beta_1 V^* I_1^*)yv \\
&- (k_2\delta_2\beta_2 V^* I_2^* - k_4\delta_2\beta_2 V^* I_2^*)yw - (k_3\beta_1 S^* I_1^* + k_3\beta_1\delta_1 V^* I_1^* - k_5 a_1 E_1^*)z \\
&- (k_4\beta_2 S^* I_2^* + k_4\beta_2\delta_2 V^* I_2^* - k_6 a_2 E_2^*)u - k_5 a_1 E_1^* \frac{z}{v} - k_6 a_2 E_2^* \frac{u}{w} \\
=:& F(x, y, z, u, v, w).
\end{aligned}
$$

Now we choose the positive constants $k_1, k_2, k_3, k_4, k_5, k_6$ as follows:

$$
k_1 = k_2 = k_3 = k_4 = 1,\ k_5 = \frac{a_1 + \mu}{a_1},\ k_6 = \frac{a_2 + \mu}{a_2}.
$$

Substituting them into the function $F(x, y, z, u, v, w)$ gives

$$
\begin{aligned}
F(x, y, z, u, v, w) = &[2\Lambda + \gamma V^* + pS^* + (a_1 + \mu)E_1^* + (a_2 + \mu)E_2^*] \\
&- \mu S^* x - \Lambda\frac{1}{x} - \mu V^* y \\
&- \gamma V^* \frac{y}{x} - pS^* \frac{x}{y} - \beta_1 S^* I_1^* \frac{xv}{z} - \delta_1\beta_1 V^* I_1^* \frac{yv}{z} - \beta_2 S^* I_2^* \frac{xw}{u} \\
&- \delta_2\beta_2 V^* I_2^* \frac{yw}{u} - (a_1 + \mu)E_1^* \frac{z}{v} - (a_2 + \mu)E_2^* \frac{u}{w} \\
=&\mu S^*\Big(2 - x - \frac{1}{x}\Big) + \gamma V^*\Big(2 - \frac{x}{y} - \frac{y}{x}\Big) + \mu V^*\Big(3 - y - \frac{1}{x} - \frac{x}{y}\Big) \\
&+ \beta_1 S^* I_1^*\Big(3 - \frac{1}{x} - \frac{xv}{z} - \frac{z}{v}\Big) + \beta_2 S^* I_2^*\Big(3 - \frac{1}{x} - \frac{xw}{u} - \frac{u}{w}\Big) \\
&+ \delta_2\beta_2 V^* I_2^*\Big(4 - \frac{1}{x} - \frac{x}{y} - \frac{yw}{u} - \frac{u}{w}\Big) \\
&+ \delta_1\beta_1 V^* I_1^*\Big(4 - \frac{1}{x} - \frac{x}{y} - \frac{yv}{z} - \frac{z}{v}\Big).
\end{aligned}
$$

Here, clearly $F(x, y, z, u, v, w) \le 0$, and the equality holds only for $x = y = 1$, $z = v$, and $u = w$, i.e.,

$$
\begin{aligned}
&\{(x, y, z, u, v, w) \in \Delta : F(x, y, z, u, v, w) = 0\} \\
&\quad \equiv \{(x, y, z, u, v, w) : x = y = 1, z = v, u = w\},
\end{aligned}
$$

which corresponds to the set

$$\Delta' = \left\{(S, V, E_1, E_2, I_1, I_2) : S = S^*, V = V^*, \frac{E_1}{E_1^*} = \frac{I_1}{I_1^*}, \frac{E_2}{E_2^*} = \frac{I_2}{I_2^*}\right\} \subset \Delta.$$

It is evident to see that the maximum invariant set on the set Δ' is the singleton $\{D^*\}$, therefore the endemic equilibrium D^* is globally stable in Δ by LaSalle's Invariance Principle (LaSalle 1976). □

3.4 Uniform persistence

Epidemiological implications of persistence mean the disease persists for a future time. Also, we can say that the disease is endemic if the infected population persists above a certain level for a sufficiently large time. For a multi-strain disease, the epidemiological consequence of persistence is that all strains persist above a certain level for a long time. Mathematically, the meaning of persistence is that strictly positive solutions do not have omega limit points on the boundary of the non-negative axes. A population $x(t)$ is called uniformly persistent if there is an $\epsilon > 0$, independent of $x(0) > 0$ such that $\lim_{t\to\infty} x(t) > \epsilon$. We say that a system persists uniformly whenever each component persists uniformly. For the persistence result of system (1), we have the following theorem:

Theorem 3.6 *The system* (1) *is uniformly persistent if* $R_1 > 1$ *and* $R_2 > 1$.

Proof The necessity of $R_1 > 1$ and $R_2 > 1$ ensues from the global stability of the equilibria D^0 and D^2 which excludes any kind of persistence of both strains when $R_1 < 1$ or $R_2 < 1$. To prove the uniform persistence, we need to show that there are no omega limit points on the axes of orbits initiating in the interior of the positive cone. Suppose v is a point in the positive cone and $\Theta(v)$ is the orbit through v and w is the omega limit set of the orbit through v. Note that $w(v)$ is bounded. We claim that D^0 and D^2 do not belong to $w(v)$. If $D^0, D^2 \in w(v)$, then by Butler-McGehee lemma (Freedman and Waltman 1985), there exists a point $u \in w(v) \cap M^s(D^0)$ and $z \in w(v) \cap M^s(D^2)$, where $M^s(D^0)$ and $M^s(D^2)$ denote the stable manifolds of D^0 and D^2, respectively. Since $\Theta(u)$ and $\Theta(z)$ lie in $w(v)$, we conclude that $\Theta(u)$ and $\Theta(z)$ are unbounded, which is a contradiction. Hence, $w(v)$ lies in the positive cone and the system (1) is persistent. Finally, since only the closed orbits and the equilirbia from the omega limit set of the solutions on the boundary of $\mathbb{R}^8_+$ and the system (1) is dissipative, by Butler et al. (1986), the system (1) is uniformly persistent. □

3.5 Bifurcations

Different dynamical behaviors may occur in a mathematical model for the variation of the model parameters. The critical parametric value at which qualitative dynamic change occurs is called a bifurcation point. The objective of this section is to determine some local bifurcations of the system (1) with the variation of different parameters.

3.5.1 Hopf bifurcation

This section focuses on the local stability and Hopf bifurcation at the positive equilibrium D^* of system (1), which represents the coexistence of the both strains (native and mutant). To determine the local asymptotic stability of D^*, the characteristic equation of the linearized system of (1) at D^* is utilized. The characteristic equation is given by

$$C(\lambda) = \lambda^7 + l_1\lambda^6 + l_2\lambda^5 + l_3\lambda^4 + l_4\lambda^3 + l_5\lambda^2 + l_6\lambda + l_7 = 0, \tag{17}$$

where $l_1, l_2, l_3, l_4, l_5, l_6$, and l_7 are given in Appendix A. Now, we define Routh-Hurwitz determinants

$$H_1 = l_1\,, \quad H_2 = \begin{vmatrix} l_1 & l_3 \\ 1 & l_2 \end{vmatrix}, \quad H_3 = \begin{vmatrix} l_1 & l_3 & l_5 \\ 1 & l_2 & l_4 \\ 0 & l_1 & l_3 \end{vmatrix}, \quad H_4 = \begin{vmatrix} l_1 & l_3 & l_5 & l_7 \\ 1 & l_2 & l_4 & l_6 \\ 0 & l_1 & l_3 & l_5 \\ 0 & 1 & l_2 & l_4 \end{vmatrix},$$

$$H_5 = \begin{vmatrix} l_1 & l_3 & l_5 & l_7 & 0 \\ 1 & l_2 & l_4 & l_6 & 0 \\ 0 & l_1 & l_3 & l_5 & l_7 \\ 0 & 1 & l_2 & l_4 & l_6 \\ 0 & 0 & l_1 & l_3 & l_5 \end{vmatrix}, \quad H_6 = \begin{vmatrix} l_1 & l_3 & l_5 & l_7 & 0 & 0 \\ 1 & l_2 & l_4 & l_6 & 0 & 0 \\ 0 & l_1 & l_3 & l_5 & l_7 & 0 \\ 0 & 1 & l_2 & l_4 & l_6 & 0 \\ 0 & 0 & l_1 & l_3 & l_5 & l_7 \\ 0 & 0 & 1 & l_2 & l_4 & l_6 \end{vmatrix}, \quad H_7 = l_7 H_6.$$

By Routh-Hurwitz criterion, D^* is locally asymptotically stable (i.e. $Re(\lambda) < 0$) if and only if $H_1 > 0, H_2 > 0, H_3 > 0, H_4 > 0, H_5 > 0, H_6 > 0$, and $H_7 > 0$; otherwise, D^* becomes unstable.

Further, we determine the occurrence conditions of Hopf bifurcation of system (1). To study the Hopf bifurcation, bifurcation parameter should be chosen at first. Among all parameters of system (1), we choose the parameter ν_1, which represents the mutation rate of the native strain. With the other parameter values given, we can calculate the threshold value of the bifurcation parameter ν_1. In the following, we denote this threshold value of Hopf bifurcation point as $\nu_1 = \nu_1^*$.

By Liu criterion (Liu 1994), we assume that there is a smooth curve of equilibrium points $(D(\nu_1), \nu_1^*)$ with $D(\nu_1) = \nu_1^*$ for system (1) and (D^*, ν_1^*) is a positive equilibrium point. If $C(\lambda, \nu_1^*) = \lambda^7 + l_1(\nu_1^*)\lambda^6 + l_2(\nu_1^*)\lambda^5 + l_3(\nu_1^*)\lambda^4 + l_4(\nu_1^*)\lambda^3 + l_5(\nu_1^*)\lambda^2 + l_6(\nu_1^*)\lambda + l_7(\nu_1^*)$ is the characteristic equation at (D^*, ν_1^*), then for a simple Hopf bifurcation, we have the following conditions:

(i) $l_7(\nu_1^*) > 0, H_1(\nu_1^*) > 0, H_2(\nu_1^*) > 0, H_3(\nu_1^*) > 0, H_4(\nu_1^*) > 0, H_5(\nu_1^*) > 0$, and $H_6(\nu_1^*) = 0$.

(ii) $\frac{d}{d\nu_1}(H_6(\nu_1^*)) \neq 0$,

where $H_1(\nu_1^*), H_2(\nu_1^*), H_3(\nu_1^*), H_4(\nu_1^*), H_5(\nu_1^*)$, and $H_6(\nu_1^*)$ are the Hurwitz determinants at the bifurcation parameter ν_1^*.

If the condition (i) holds, then the characteristic polynomial have to meet the condition for a pair of purely imaginary eigenvalues. Now for the occurrence of Hopf

bifurcation, we need to derive the transversality condition (ii). For this, we let $\pm i\omega$ be a pair of purely imaginary eigenvalues. Here, differentiating the characteristic equation (17) with respect to ν_1, we obtain

$$(7\lambda^6 + 6l_1\lambda^5 + 5l_2\lambda^4 + 4l_3\lambda^3 + 3l_4\lambda^2 + 2l_5\lambda + l_6)\frac{d\lambda}{d\nu_1} + \lambda^6\frac{dl_1}{d\nu_1} + \lambda^5\frac{dl_2}{d\nu_1} + \lambda^4\frac{dl_3}{d\nu_1} + \lambda^3\frac{dl_4}{d\nu_1} + \lambda^2\frac{dl_5}{d\nu_1} + \lambda\frac{dl_6}{d\nu_1} + \frac{dl_7}{d\nu_1} = 0.$$

Further, we obtain

$$\left(\frac{d\lambda}{d\nu_1}\right)^{-1} = -\frac{7\lambda^6 + 6l_1\lambda^5 + 5l_2\lambda^4 + 4l_3\lambda^3 + 3l_4\lambda^2 + 2l_5\lambda + l_6}{\lambda^6\frac{dl_1}{d\nu_1} + \lambda^5\frac{dl_2}{d\nu_1} + \lambda^4\frac{dl_3}{d\nu_1} + \lambda^3\frac{dl_4}{d\nu_1} + \lambda^2\frac{dl_5}{d\nu_1} + \lambda\frac{dl_6}{d\nu_1} + \frac{dl_7}{d\nu_1}}.$$

Furthermore, we have

$$\begin{aligned} sign\left[\frac{d(Re(\lambda))}{d\nu_1}\right]_{\lambda=i\omega, H_6=0} &= sign\left[Re\left(\frac{d\lambda}{d\nu_1}\right)^{-1}\right]_{\lambda=i\omega, H_6=0} \\ &= sign[\Upsilon], \end{aligned}$$

where,

$$\begin{aligned} \Upsilon &= Re\left[\frac{(7\omega^6 - 5l_2\omega^4 + 3l_4\omega^2 - l_6) + i(-6l_4\omega^5 + 4l_3\omega^2 - 2l_5\omega)}{(-\omega^6\frac{dl_1}{d\nu_1} + \omega^4\frac{dl_3}{d\nu_1} - \omega^2\frac{dl_5}{d\nu_1} + \frac{dl_7}{d\nu_1}) + i(\omega^5\frac{dl_2}{d\nu_1} - \omega^3\frac{dl_4}{d\nu_1} + \omega\frac{dl_6}{d\nu_1})}\right] \\ &= \frac{M_1M_3 + M_2M_4}{M_3^2 + M_4^2}, \\ M_1 &= 7\omega^6 - 5l_2\omega^4 + 3l_4\omega^2 - l_6, \quad M_2 = -6l_4\omega^5 + 4l_3\omega^2 - 2l_5\omega, \\ M_3 &= -\omega^6\frac{dl_1}{d\nu_1} + \omega^4\frac{dl_3}{d\nu_1} - \omega^2\frac{dl_5}{d\nu_1} + \frac{dl_7}{d\nu_1}, \quad M_4 = \omega^5\frac{dl_2}{d\nu_1} - \omega^3\frac{dl_4}{d\nu_1} + \omega\frac{dl_6}{d\nu_1}. \end{aligned}$$

If $M_1M_3 + M_2M_4 > 0$, then $sign\left[\frac{d(Re(\lambda))}{d\nu_1}\right]_{\nu_1=\nu_1^*} > 0$ and the transversality condition (ii) holds. Summarizing the above discussion, we obtain the subsequent theorem:

Theorem 3.7 *For the existing positive equilibrium D^* of system (1), if the conditions (i) and (ii) hold, then the system (1) around D^* enters into Hopf bifurcation when ν_1 crosses through ν_1^*.*

3.5.2 Transcritical bifurcation

We see that Eq. (6) has a zero eigenvalue when either $R_1 = 1$ or $R_2 = 1$. Thus, the system (1) may undergo a transcritical bifurcation at D^0 when either $R_1 = 1$ or $R_2 = 1$. In this subsection, we establish conditions on the parameters using Theorem 4.1 from Castillo-Chavez and Song (2004) and center manifold theory (Gukenheimer and Holmes 1983). For the transcritical bifurcation, we establish the following theorem:

Theorem 3.8 *1. Assume $R_1 < 1$, the system (1) undergoes a transcritical bifurcation near D^0, when $R_2 = 1$.*
2. Assume $R_2 < 1$, the system (1) undergoes a transcritical bifurcation near D^0, when $R_1 = 1$.

Proof 1. We choose β_2 as a bifurcation parameter. By solving $R_2 = 1$, we obtain

$$\beta_2 = \beta_2^* = \frac{\mu\,(a_2+\mu)\,(\alpha_2+d_2+\mu)\,(\gamma+\mu+p)}{a_2\Lambda\,(\gamma+\mu+\delta_2 p)}.$$

It can easily be obtained that the Jacobian $J_{(D^0,\beta_2^*)}$ evaluated at D^0 and $\beta_2 = \beta_2^*$ has a simple zero eigenvalue and other eigenvalues have negative sign. Hence D^0 is a non-hyperbolic equilibrium, when $\beta_2 = \beta_2^*$. Now, we calculate a right eigenvector $W = (w_1, w_2, w_3, w_4, w_5, w_6)$ and a left eigenvector $V = (v_1, v_2, v_3, v_4, v_5, v_6)$ associated to the zero eigenvalue. Here

$$\begin{aligned}
w_1 &= -\frac{(a_2+\mu)\,(\alpha_2+d_2+\mu)\left((\gamma+\mu)^2+\gamma\delta_2 p\right)}{a_2\mu(\gamma+\mu+p)\,(\gamma+\mu+\delta_2 p)},\\
w_2 &= -\frac{p\,(a_2+\mu)\,(\alpha_2+d_2+\mu)\,(\gamma+\mu+\delta_2(\mu+p))}{a_2\mu(\gamma+\mu+p)\,(\gamma+\mu+\delta_2 p)},\\
w_3 &= 0, \quad w_4 = \frac{\mu+d_2+\alpha_2}{a_2}, \quad w_5 = 0, \quad w_6 = 1, \quad w_7 = 0,\\
v_1 &= 0, \quad v_2 = 0, \quad v_3 = \frac{a_1\nu_1}{(\mu+a_1)(\mu+d_1+\alpha_1+\nu_1)(1-R_1)},\\
v_4 &= 1, \quad v_5 = \frac{\nu_1}{(\mu+d_1+\alpha_1+\nu_1)(1-R_1)}, \quad v_6 = 1, \quad v_7 = 0.
\end{aligned}$$

Now from Theorem 4.1 of Castillo-Chavez and Song (2004), we need to calculate the bifurcation constants a and b. For system (1), a and b with the associated non-zero partial derivatives of f (evaluated at D^0, $x_1 = S, x_2 = V, x_3 = E_1, x_4 = E_2, x_5 = I_1, x_6 = I_2, x_7 = R_1$) are given by

$$\begin{aligned}
a &= 2v_3w_1w_5\frac{\partial^2 f_3}{\partial S\partial I_1} + 2v_3w_2w_5\frac{\partial^2 f_3}{\partial V\partial I_1} + 2v_4w_1w_6\frac{\partial^2 f_4}{\partial S\partial I_2}\\
&\quad + 2v_4w_2w_6\frac{\partial^2 f_4}{\partial V\partial I_2} + 2v_4w_6w_7\frac{\partial^2 f_4}{\partial I_2\partial R_1}\\
&= 2v_4w_6(w_1+\delta_2 w_2)\beta_2^* < 0,\\
b &= 2v_4w_6\frac{\partial^2 f_4}{\partial\beta_2\partial I_2} = 2v_4w_6(S^0+\delta_2 V^0) > 0.
\end{aligned}$$

Since the coefficient a is negative and b is positive, the direction of the bifurcation of system (1) at $\beta_2 = \beta_2^*$ is forward.

2. By choosing β_1 as a bifurcation parameter and solving $R_1 = 1$, we obtain

$$\beta_1 = \beta_1^* = \frac{\mu\,(a_1+\mu)\,(\gamma+\mu+p)\,(\alpha_1+d_1+\mu+\nu_1)}{a_1\Lambda\,(\gamma+\mu+\delta_1 p)}.$$

Following simple procedure of previous case, we obtain that D^0 is a non-hyperbolic equilibrium, when $\beta_1 = \beta_1^*$. Now, we calculate a right eigenvector $W_1 = (w_{11}, w_{22}, w_{33}, w_{44}, w_{55}, w_{66})$ and a left eigenvector $V_1 = (v_{11}, v_{22}, v_{33}, v_{44}, v_{55}, v_{66})$ associated to the zero eigenvalue. Here

$$\begin{aligned}
w_{11} &= -\frac{\Lambda\beta_2((\gamma+\mu)^2+p\gamma\delta_2)\nu_1}{\alpha_1\mu(p+\gamma+\mu)^2(\mu+d_2+\alpha_2)(\mu+a_2)(1-R_2)}\\
&\quad - \frac{(a_1+\mu)\,(\alpha_1+d_1+\mu+\nu_1)\left((\gamma+\mu)^2+\gamma\delta_1 p\right)}{a_1\alpha_1(\gamma+\mu+p)\,(\gamma+\mu+\delta_1 p)},\\
w_{22} &= -\frac{p(\gamma+\mu+(p+\mu)\delta_2)}{(p+\gamma+\mu)\alpha_1}\Big(\frac{\Lambda\beta_2\nu_1}{\mu(p+\gamma+\mu)(\mu+d_2+\alpha_2)(1-R_2)}\\
&\quad + \frac{(\mu+a_1)(\mu+d_1+\alpha_1+\nu_1)}{a_1(\gamma+\mu+p\delta_2)}\Big),\\
w_{33} &= \frac{\mu\,(\alpha_1+d_1+\mu+\nu_1)}{a_1\alpha_1},\\
w_{44} &= \frac{\Lambda\beta_2(\gamma+\mu+p\delta_2)\nu_1}{\alpha_1(p+\gamma+\mu)(\mu+d_2+\alpha_2)(\mu+a_2)(1-R_2)}, \quad w_{55} = \frac{\mu}{\alpha_1},\\
w_{66} &= \frac{\mu\nu_1}{\alpha_1(\mu+d_2+\alpha_2)(1-R_2)}, \quad w_{77} = 1 \quad v_{11} = 0, \quad v_{22} = 0,\\
v_{33} &= \frac{a_1}{a_1+\mu}, \quad v_{44} = 0,\\
v_{55} &= 1, \quad v_{66} = 0, \quad v_{77} = 0.
\end{aligned}$$

Similarly, as in previous case, we have

$$\begin{aligned}
a &= 2v_{33}w_{11}w_{55}\frac{\partial^2 f_3}{\partial S\partial I_1} + 2v_{33}w_{22}w_{55}\frac{\partial^2 f_3}{\partial V\partial I_1}\\
&= 2v_{33}w_{11}w_{55}\beta_1^* + 2v_{33}w_{22}w_{55}\delta_1\beta_1^*,\\
&= 2v_{33}w_{55}\beta_1^*(w_{11}+\delta_1 w_{22}) < 0,\\
b &= 2v_{33}w_{55}\frac{\partial^2 f_3}{\partial\beta_1\partial I_1} = 2v_{33}w_{55}(S^0+\delta_1 V^0) > 0.
\end{aligned}$$

Therefore again in this case, the direction of the bifurcation of system (1) at $\beta_1 = \beta_1^*$ is forward. □

4 Implications for disease control

For vaccine-preventable diseases, not all susceptible individuals can be immunized due to various reasons. These include being too young (as vaccination may be harmful to infants or young children), having weakened immune systems or underlying health conditions (where vaccination could worsen their prognosis), advanced age, or personal reasons based on religion, tradition, or culture. However, the key question is: what is the minimum proportion of individuals we need to vaccinate in order to protect those who cannot be vaccinated from severe disease or death? The idea of herd immunity in the disease dynamics is related to the indirect protection against acquiring of infectious disease, which members of the community obtain when a large percentage of the populace has become protected to the contagious disease due to natural recovery from prior infection or vaccination (Anderson 1992; Anderson and May 1985; Elbasha and Gumel 2021). The outcome of herd immunity is that persons who are not immune (e.g., those who have not been infected yet or cannot be vaccinated) obtain some defense against acquiring the infection. The fastest and safest way to attain herd immunity is vaccination. It should, however, be stated that Sweden implemented the other procedure for achieving herd immunity in the COVID-19 dynamics in Sweden (Friedman 2020). In other words, the Swedish public health agencies aimed to achieve herd immunity without implementing common strategies like community lockdowns, social distancing, contact tracing, or the widespread use of face masks in public. Instead, they chose to allow individuals to contract the disease and hopefully recover from it. In this section, a theoretical condition for achieving community-wide vaccine-induced herd immunity is obtained. Theorem 3.3 has significant public health implications. It reveals that if the imperfect vaccine has sufficient efficacy and coverage rate to make $R_0 < 1$, COVID-19 will be eradicated from society. The global stability of the disease-free equilibrium (Theorem 3.3) for $R_0 < 1$ confirms that such epidemics do not hit. This means R_0 is an appropriate combination of parameters to measure the efficiency of a vaccination campaign.

4.1 Herd immunity

Not every person in a given population expects to be immunized in order to eradicate the disease. A fraction of people with immunity in the given population is required to stop an epidemic is named herd immunity. Let ρ denotes the fraction of the vaccinated population at D^0 (the disease-free equilibrium). Then,

$$\rho = \frac{p}{\mu + \gamma + p}.$$

In the absence of vaccination, i.e., when $p = 0$, the basic reproduction number is given by R_{0wv}. Hence, we can write

$$R_0 = \max\left\{R_{1wv}(1 - (1 - \delta_1)\rho),\, R_{2wv}(1 - (1 - \delta_2)\rho)\right\}, \tag{18}$$

with $R_1 = R_{1wv}(1-(1-\delta_1)\rho)$, and $R_2 = R_{2wv}(1-(1-\delta_2)\rho)$. It is noted that $R_1 \leq R_{1wv}$, $R_2 \leq R_{2wv}$, and thus $R_0 \leq R_{0wv}$. The equality holds only when $\rho = 0$ (i.e., $p = 0$) or $\delta_1 = \delta_2 = 1$. This indicates that the vaccine, even not 100% effective, will certainly reduce the basic reproduction number of the disease. Since $R_0 < 1$ is a necessary and sufficient condition for the eradication of disease (Theorem 3.3), hence it follows from (18) that

$$\rho > \max\left\{\frac{1}{1-\delta_1}\left(1-\frac{1}{R_{1wv}}\right), \frac{1}{1-\delta_2}\left(1-\frac{1}{R_{2wv}}\right)\right\} = \rho_{critical} \tag{19}$$

is also a necessary and sufficient condition for disease elimination. Here $\rho_{critical}$ signifies herd immunity. Although this outcome could be achieved in the case of continuous vaccination and that herd immunity is attained if the vaccination rate is large enough such that ρ, the fraction of vaccinated individuals at the disease-free equilibrium, exceeds the critical value $\rho_{critical}$. From Theorem 3.3, we obtain the following consequence:

Proposition 4.1 *COVID-19 can be eradicated from the population if* $\rho > \rho_{critical}$.

The inequality (19) can be expressed in terms of the vaccination rate p. This is done by noting, first of all, that R_0 is a decreasing function of p,

$$\frac{dR_0}{dp} = \max\left\{\frac{-\Lambda(\gamma+\mu)(1-\delta_1)a_1\beta_1}{\mu(p+\gamma+\mu)^2(\mu+a_1)(\mu+d_1+\alpha_1+\nu_1)}, \frac{-\Lambda(\gamma+\mu)(1-\delta_2)a_2\beta_2}{\mu(p+\gamma+\mu)^2(\mu+a_2)(\mu+d_2+\alpha_2)}\right\} < 0$$

and so it is minimized if p becomes sufficiently large enough. Taking the limit as p approaches infinity, we observe that this expression is always greater than $\max\{\delta_1 R_{1wv}, \delta_2 R_{2wv}\}$. Thus, if $\max\{\delta_1 R_{1wv}, \delta_2 R_{2wv}\} > 1$, then no amount of vaccination can make R_0 smaller than unity. Alternatively, if $\max\{\delta_1 R_{1wv}, \delta_2 R_{2wv}\} < 1$, then the condition

$$p > \max\left\{\frac{(\gamma+\mu)(R_{1wv}-1)}{1-\delta_1 R_{1wv}}, \frac{(\gamma+\mu)(R_{2wv}-1)}{1-\delta_2 R_{2wv}}\right\} = p_{critical} \tag{20}$$

gives $R_0 < 1$. Of course, this condition assumes $R_0 > 1$, since disease elimination follows without vaccination if $R_0 < 1$ (by Theorem 3.3 and the fact that $R_0 \leq R_{0wv}$). It is easy to show that from (20), we obtain $R_0 < 1$ if $p > p_{critical}$, and $R_0 > 1$ if $p < p_{critical}$. Thu, we have the following result:

Proposition 4.2 *If* $\max\{\delta_1 R_{1wv}, \delta_2 R_{2wv}\} < 1$ *and* $p > p_{critical}$, *then COVID-19 will be eliminated from the community. If* $\max\{\delta_1 R_{1wv}, \delta_2 R_{2wv}\} > 1$, *then no amount of vaccination would be able to prevent the COVID-19 outbreak in the community.*

Table 2 Numerical values of parameters

Parameters	Value with unit	Reference
Λ	10,000 people per week	Assumed
β_1	0.000001	Assumed
β_2	0.0000003	Assumed
p	0.02 week^{-1}	Assumed
μ	0.0003 week^{-1}	$1/(65 \times 48)$
$1-\delta_1$	0.75 (dimensionless)	Assumed that vaccine efficacy is 75% against native strain
$1-\delta_2$	0.40 (dimensionless)	Assumed that vaccine efficacy is 40% against mutant strain
γ	1/32 week^{-1}	Assumed that loss of immunity of vaccinated individuals after 32 weeks
a_1	1 week^{-1}	Incubation (1 Week) Lauer et al. (2020)
a_2	1 week^{-1}	Incubation (1 Week) Lauer et al. (2020)
α_1	1/2 week^{-1}	Recovery (2 Weeks) Iboi et al. (2020)
α_2	1/2 week^{-1}	Recovery (2 Weeks) Iboi et al. (2020)
d_1	0.0006 week^{-1}	Assumed
d_2	0.0006 week^{-1}	Assumed
$1-\delta_3$	0.90 (dimensionless)	Assumed that recovered individuals have 90% immunity against mutant strain
ν_1	0.3 week^{-1}	Assumed

5 Numerical illustration

In this section, we investigate the dynamics of system (1) numerically for different sets of parametric values. Such investigations aim to determine the effect of varying the values of the different parameters and support the obtained theoretical results. It is observed that the hypothetical values of parameters given in Table 2 are biologically feasible. However, to verify the bifurcations and different dynamical behavior of system (1), some parameters are varied differently from Table 2.

The dynamics of system (1) is simulated using MATLAB 2018a. Figure 2a shows that for $R_0 = \max\{R_1, R_2\} = 0.9735 < 1$, DFE ($D^0$) is asymptotically stable. Figure 2b represents that the mutant dominant equilibrium (D^2) is asymptotically stable for $R_1 < 1$ and $R_2 > 1$. Further, Fig. 3 shows that mutation rate (ν_1) changes the dynamics of positive equilibrium of system (1). Figure 3a represents that the positive equilibrium is asymptotically stable. Figure 3b, c ensure that system (1) loses its stability around the positive equilibrium for high mutation rate and periodic solutions occur. Furthermore, Fig. 3d shows that the positive equilibrium regains its stability for further higher mutation rate. This type of dynamics is called endemic bubble (Liu et al. 2015).

Figures 4a, b depict the transcritical bifurcation diagrams with respect to R_2 and R_1, respectively, as the results obtained in Theorem 3.8. Figure 4a shows that system

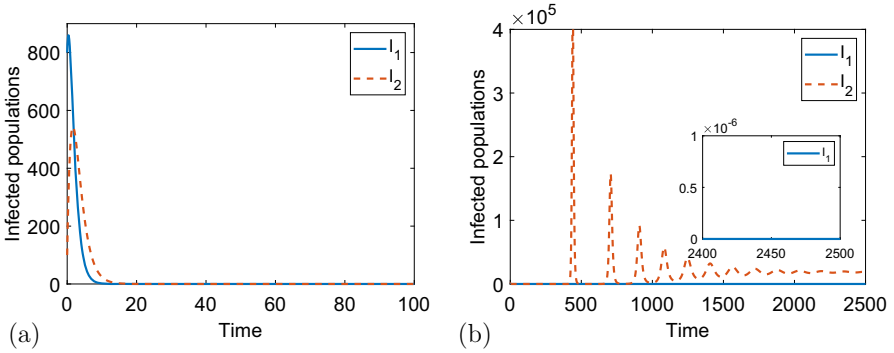

Fig. 2 **a** The solutions I_1 and I_2 of system (1) for the parametric values $\beta_1 = 0.000000033$, $\beta_2 = 0.000000017$, and others from Table 2. **b** The solutions I_1 and I_2 of system (1) for $\beta_1 = 0.0000000033$, $\beta_2 = 0.0000003$, and other parametric values from Table 2

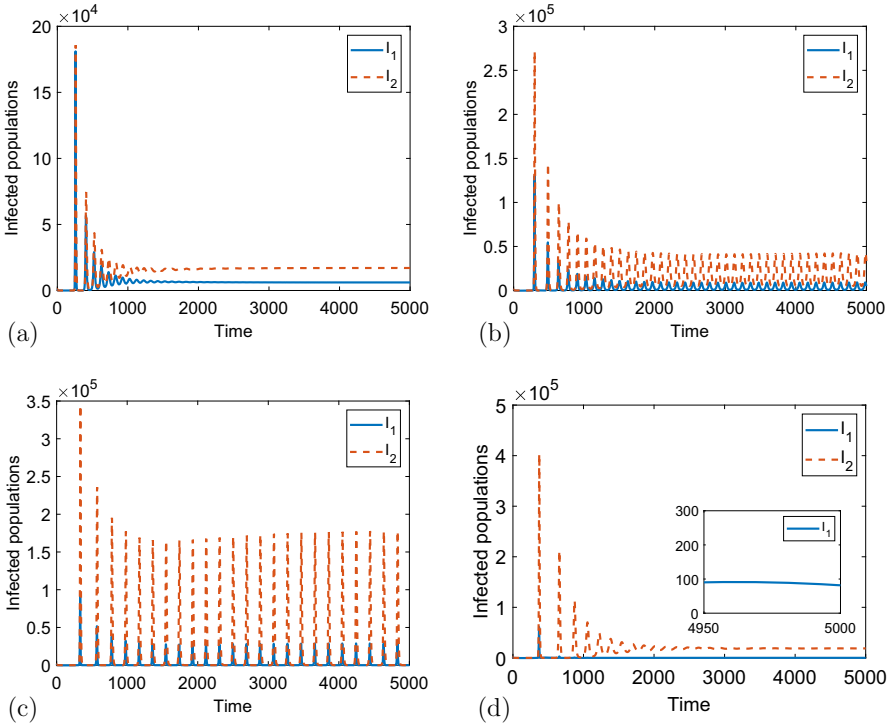

Fig. 3 **a** The solutions I_1 and I_2 of system (1) for the parametric values in Table 2 and $\nu_1 = 0.3$. **b** The solutions I_1 and I_2 of system (1) for $\nu_1 = 0.5$. **c** The solutions I_1 and I_2 of system (1) for $\nu_1 = 0.7$. **d** The solutions I_1 and I_2 of system (1) for $\nu_1 = 0.90$

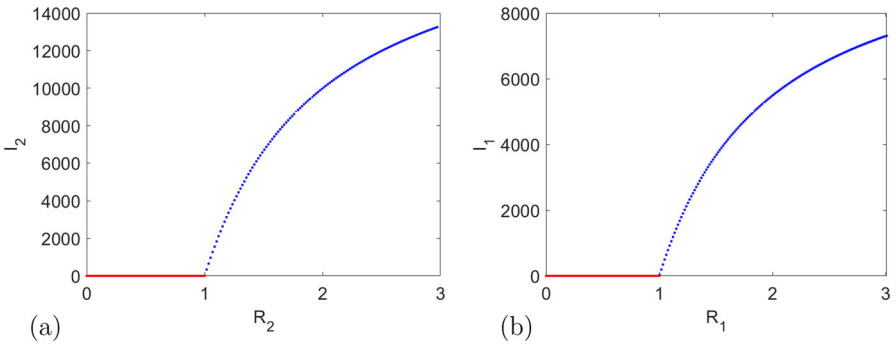

Fig. 4 **a** Transcritical bifurcation with respect to R_2 when $R_1 < 1$. The blue curve shows the stable mutant dominant equilibrium when $R_2 > 1$. **b** Transcritical bifurcation with respect to R_1 when $R_2 < 1$. The blue curve shows the stable endemic equilibrium (only native strain exists, i.e. $I_2 = 0$) when $R_1 > 1$. Red colored curve shows the disease-free equilibrium (color figure online)

(1) undergoes a transcritical bifurcation at $R_2 = 1$ and exchanges the stability between disease free equilibrium (D^0) and mutant dominant equilibrium (D^2). For this scenario, native strain is assumed to die out, i.e. $I_1 = 0$ when $R_1 < 1$. More precisely, D^0 is stable when $R_2 < 1$, while a unique stable mutant dominant equilibrium (D^2) appears and D^0 becomes unstable when $R_2 > 1$. The equilibrium D^2 exists and stable when $R_2 > 1$ and $R_1 < 1$ which has also been theoretically proved in Sect. 3.2 and Theorem 3.8. Figure 4b illustrates that system (1) exchanges the stability between disease free equilibrium (D^0) and native strain's associated endemic equilibrium at $R_1 = 1$ implying that system (1) undergoes a transcritical bifurcation at $R_1 = 1$. This scenario happens when mutant strain is assumed to die out for $R_2 < 1$. When mutant strain dies out only native strain's associated endemic equilibrium exists and stable when $R_1 > 1$. We have not computed an explicit expression for native strain's associated endemic equilibrium, it can simply be computed by considering a simple SVEIR model by considering $I_2 = 0$.

Furthermore, Fig. 5 shows the endemic equilibrium (D^*) is locally asymptotically stable for small and large enough values of ν_1, but unstable for intermediate values of ν_1. In this way, we get the bifurcation diagram in Fig. 5, which we call an endemic bubble. As shown in the bifurcation diagram (Fig. 5), for a lower range of values of ν_1, both strains persist in the environment and system (1) is asymptotically stable. For a range of ν_1, the periodic oscillations (limit cycle) will appear, but for higher values of ν_1, system (1) regains its stability. Figure 6 illustrates the Hopf bifurcation diagram with respect to the parameter δ_3. It shows that the system (1) is locally asymptotically stable for lower values of δ_3 and periodic solutions (Hopf bifurcation) appear for higher values of δ_3.

6 Case study on COVID-19 data in India

Here we estimate the unknown parameters of the system (1) on the cumulative cases and deaths of COVID-19 in India from March 1, 2021 to September 27, 2021 by using

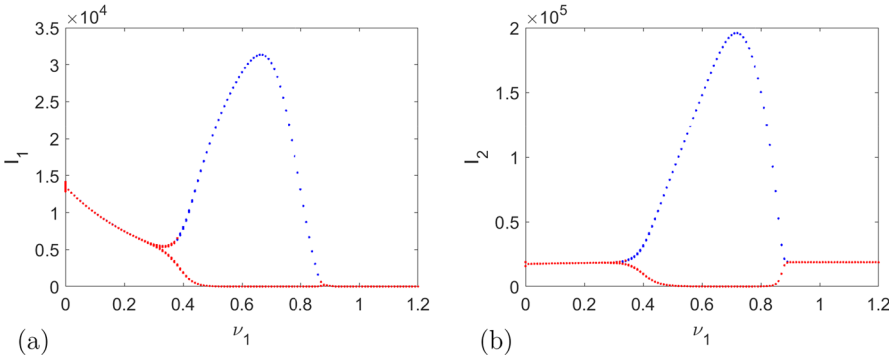

Fig. 5 Bifurcation diagrams (endemic bubble) with respect to mutation rate (ν_1), other parametric values remain same as in Table 2. The blue color shows the upper limit of the limit cycle and red color shows the lower limit of the limit cycle (color figure online)

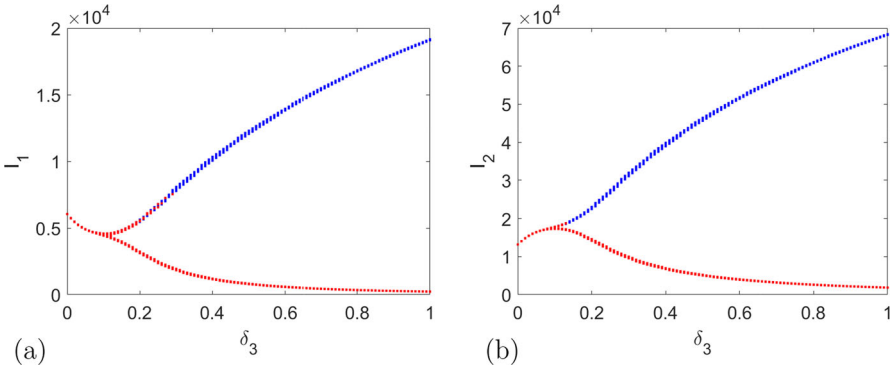

Fig. 6 Hopf bifurcation diagrams with respect to δ_3. We keep $\nu_1 = 0.4$ and other parametric values same as in Table 2. The blue color shows the upper limit of the limit cycle and red color shows the lower limit of the limit cycle (color figure online)

the MCMC algorithm (Haario et al. 2006, 2001; Ahmed 2008). We collect the data of cumulative cases and deaths of COVID-19 for March 1, 2021 to September 27, 2021 (31 weeks) from the WHO website (World Health Organization 2021a). By estimating the parameters, we estimate the mean values, standard deviation, and Geweke values of some parameters of the system (1). The cumulative cases can be given as

$$\frac{dC}{dt} = a_1 E_1 + a_2 E_2, \tag{21}$$

where $C(t)$ represents the cumulative cases, and the cumulative deaths can be given as

$$\frac{dD}{dt} = d_1 I_1 + d_2 I_2, \tag{22}$$

where $D(t)$ represents the cumulative deaths.

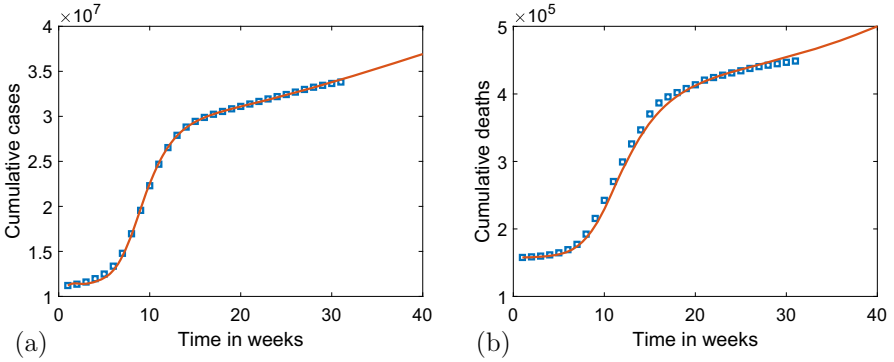

Fig. 7 Fitting results of the cumulative cases and deaths of COVID-19. **a** The blue solid boxes represent the actual reported cumulative cases and the orange curve represents the model output. **b** Blue solid boxes represent the actual reported cumulative deaths and orange curve represents the model output. For the different colors in the Figure, refer to the web version of the paper (color figure online)

In this section, we are interested in understanding the qualitative and quantitative impact of imperfect vaccine and mutation on the dynamics of COVID-19, where mutant strain is more transmissible. In particular, we consider the data of COVID-19 in India from March 1, 2021 to September 27, 2021 and in this period the delta variant was the variant of concern (VOC) and led a specific wave which was primarily identified in India in October 2020 (World Health Organization 2021d; Duong et al. 2022). The Delta variant was highly infectious, estimated to be more than double that of the previous variants (How Dangerous Is the Delta Variant 2023; Duong et al. 2022). Thus, we consider $\beta_1 < \beta_2$, specifically $\beta_2 = 2\beta_1$. However, the general methodology and mathematical could be applied to other SARS-CoV-2 variants and may be assumed $\beta_2 = \kappa\beta_1$, where $\kappa > 0$ depends on the uncertainty in the transmissibility of the mutant SARS-CoV-2 variant. We use MCMC method for 20,000 simulations to fit the Eqs. (21) and (22) and estimate the parameters. Figure 7 represents a good fitting between the cumulative reported cases of COVID-19 and the model solution, well suggesting the epidemic trend in India. Some of the parameters of the system (1) are taken either from the literature or presumed based on publicly-available COVID-19 associated information. We assume parametric values of α_1, α_2, μ, δ_1, δ_2, and δ_3 same as given in Table 2 and initial conditions given in Table 4.

By using MCMC method, we acquire the values of the parameters β_1, β_2, ν_1, d_1, and d_2 with MCMC chain of the time evolution of the cumulative cases and deaths and comparison with the confirmed cases of COVID-19 in India. We compute the mean values, standard deviation, and Geweke values of these parameters (refer in Table 3).

6.1 The effects of different efficacies of vaccine and mutation rate on cumulative cases and cumulative deaths over time

The system (1) is simulated to assess the population-level impact of the imperfect anti-COVID-19 vaccine in India. The population-level impact of the vaccine efficacy against both strains (native and mutant) on the burden of the pandemic is examined.

Table 3 Estimated values of parameters by MCMC method

Parameters	Mean value	Standard deviation	Geweke value	Reference
Λ	320000	–	–	Assumed
β_1	1.999e−07	5.3206e−13	0.99	MCMC
β_2	3.9980e−07	3.145e−13	0.99	MCMC
p	0.01	–	–	Paul et al. (2022)
γ	0.04	–	–	Bugalia et al. (2023) and Chowdhury et al. (2022)
ν_1	0.02	3.265e−04	0.98	MCMC
d_1	0.007	5.347e−05	0.99	MCMC
d_2	0.007	3.016e−05	0.99	MCMC
a_1	0.5	–	–	Assumed
a_2	0.33	–	–	Assumed

Table 4 Initial conditions for system (1) with respect to COVID-19 in India

S(0)	V(0)	$E_1(0)$	$E_2(0)$	$I_1(0)$	$I_2(0)$	$R_1(0)$	$R_2(0)$
23×10^5	12256337	10×10^4	60×10^4	10×10^3	80×10^3	60×10^2	20×10^3

Firstly, we consider different values of the vaccine efficacy against the native strain. The system (1) is then simulated using the baseline parameter values in Table 2, 3, and different values of the vaccine efficacy $(1 - \delta_1)$ against the native strain. The results obtained from the Fig. 8a show that, for the vaccine efficacy $(1-\delta_1) = 75\%$ (assumed), 34,149,900 cumulative cases (the red curve) have been reported by September 27, 2021. Predictions show that the cumulative cases would be recorded 36,923,800, by November 29, 2021 (9 weeks after September 27, 2021). The simulations further ensure a reduction with increasing values of the vaccine efficacy $(1 - \delta_1)$ from its baseline value. In particular, if we consider the vaccine efficacy as $(1-\delta_1) = 90\%$, then 36,774,900 cumulative cases would be recorded by November 29, 2021, representing only 0.40% reduction. Figure 8b represents that for the vaccine efficacy $(1-\delta_2) = 40\%$ (assumed) against the mutant strain, 34,066,700 cumulative cases (the yellow curve) have been reported by September 27, 2021. Predictions show that the cumulative cases would be recorded 36,890,600, by November 29, 2021. These simulations ensure that initially an increase in the vaccine efficacy against the mutant strain $(1 - \delta_2)$ reduces the cumulative cases but not for longer time.

The system (1) is simulated for different values of $1 - \delta_3$ (immunity against mutant strain). Figure 8c represents that, if recovered individuals by native strain have 90% immunity against mutant strain (i.e. $(1 - \delta_3) = 90\%$) (assumed), 34,149,900 cumulative cases (the blue curve) have reported by September 27, 2021. Simulations also show that the cumulative cases would be recorded 36,923,800, by November 29, 2021. These simulations observe an increase in the cumulative cases with decreasing value of $1 - \delta_3$. Particularly, if we consider $(1 - \delta_3) = 75\%$, then 37,032,000 cumulative cases would be recorded by November 29, 2021. This represents 0.29% increase in the

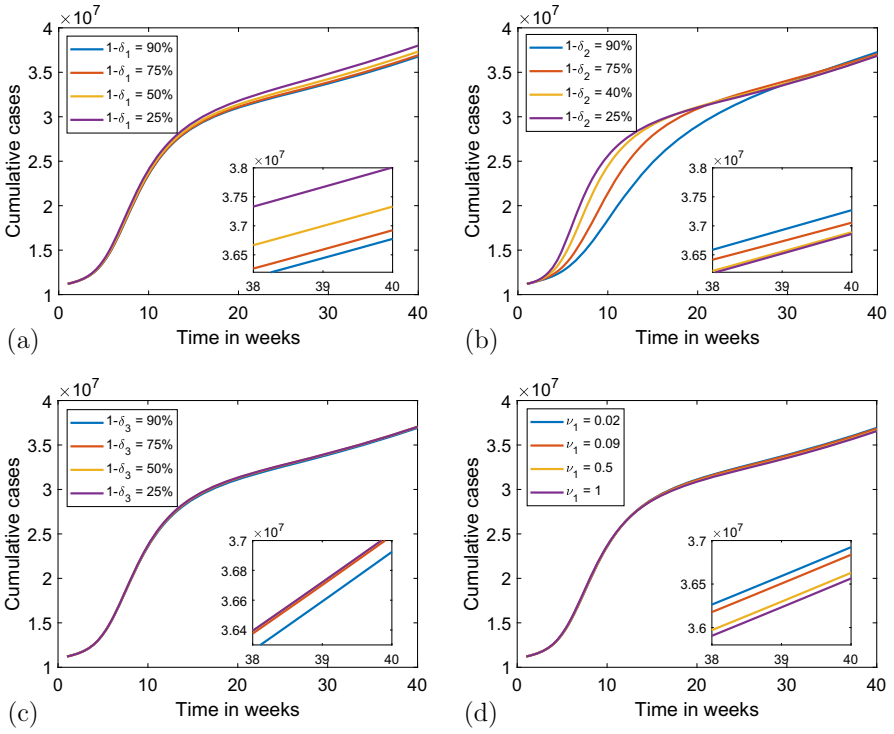

Fig. 8 Assessment of the impacts of different parameters on the cumulative cases of COVID-19 in India. Simulations of the system (1) show the cumulative cases of COVID-19 in India, as a function of time, **a** for different values of vaccine efficacy against native strain $(1-\delta_1)$. **b** for different values of vaccine efficacy against mutant strain $(1-\delta_2)$. **c** for different values of immunity against mutant strain $(1-\delta_3)$. **d** for different values of mutation rate (ν_1). The baseline parameter values are used from Tables 2 and 3

cumulative cases. If we consider $(1-\delta_3) = 50\%$, then 37,048,600 cumulative cases would be recorded by November 29, 2021, representing 0.33% increase in the cumulative cases. Furthermore, if $(1-\delta_3) = 25\%$, then 37,049,500 cumulative cases would be recorded by November 29, 2021, representing 0.34% increase in the cumulative cases.

Furthermore, simulations are also carried out to assess the impact of mutation rate on the disease dynamics of COVID-19. Figure 8d represents that, for the baseline value of the mutation rate ($\nu_1 = 0.02$), 34,149,900 cumulative cases (blue curve) have reported by September 27, 2021. Simulations show that the cumulative cases would be 36,923,800 by November 29, 2021. These simulations show a decrease in the cumulative cases with increasing values of ν_1. Particularly, if we consider $\nu_1 = 0.5$, then 36,628,700 cumulative cases would be recorded by November 29, 2021. This represents a 0.79% decrease in the cumulative cases. Furthermore, if $\nu_1 = 1$, then 36,564,100 cumulative cases would be recorded by November 29, 2021, representing 0.97% decrease in the cumulative cases.

Furthermore, the impact of vaccine efficacies on cumulative deaths is examined. The result in Fig. 9a shows that for the vaccine efficacy $(1-\delta_1) = 75\%$ (assumed), 468,197

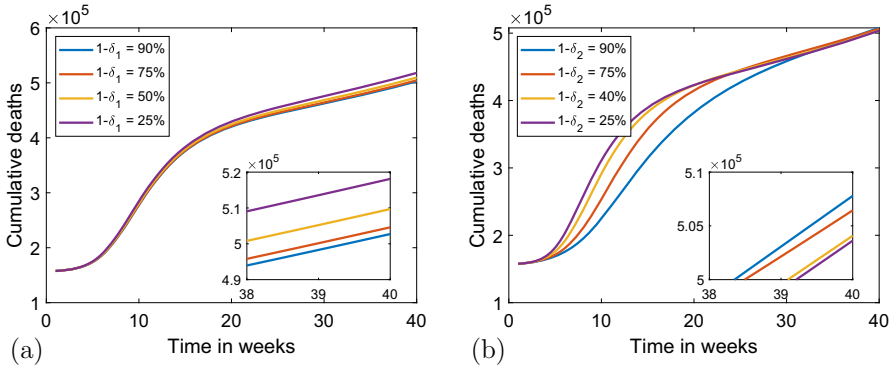

Fig. 9 Assessment of the impacts of different parameters on the cumulative deaths of COVID-19 in India. Simulations of the system (1) show the cumulative deaths of COVID-19 in India, as a function of time, **a** for different values of vaccine efficacy against native strain $(1-\delta_1)$; **b** for different values of vaccine efficacy against mutant strain $(1-\delta_2)$. The baseline parameter values are used from Tables 2 and 3

cumulative deaths (red curve) have been reported by September 27, 2021. Predictions show that the cumulative deaths would be recorded as 504,977 by November 29, 2021 (9 weeks after September 27, 2021). The simulations further show a reduction in cumulative deaths with increasing values of the vaccine efficacy $(1-\delta_1)$ from its baseline value. In particular, if we consider the vaccine efficacy as $(1-\delta_1) = 90\%$, then 502,946 cumulative deaths would be recorded by November 29, 2021, representing only a 0.4% reduction. Figure 9b represents that, for the vaccine efficacy $(1-\delta_2) = 40\%$ (assumed) against the mutant strain, 467,005 cumulative deaths (yellow curve) have been reported by September 27, 2021. Simulations show that the cumulative deaths would be recorded at 504,392 by November 29, 2021. Further predictions show that initially increasing values of the vaccine efficacy $(1-\delta_2)$ reduce the cumulative deaths but not for long time.

To examine the dependence of the end time (November 29, 2021) of the epidemic on the vaccine efficacies against both native and mutant strains, i.e. $(1-\delta_1)$, $(1-\delta_2)$, mutation rate (ν_1), and immunity against mutant strain $(1-\delta_3)$, we sketch the contour plots of the total number of the cumulative cases of COVID-19, with respect to $(1-\delta_1)$ and $(1-\delta_2)$ in Fig. 10a; $(1-\delta_3)$ and ν_1 in Fig. 10b; $(1-\delta_2)$ and ν_1 in Fig. 10c; $(1-\delta_2)$ and $(1-\delta_3)$ in Fig. 10d, respectively. In order to assess the combined impact of the parameters, the other parameters remain fixed when we vary two parameters. The results indicate that increasing the vaccine efficacies $(1-\delta_1)$ and $(1-\delta_2)$, the cumulative cases would be reduced (Fig. 10a). It can also be observed that the vaccine efficacy against the native strain $(1-\delta_1)$ is more influential than the vaccine efficacy against the mutant strain $(1-\delta_2)$, in controlling the total number of cases. In the same way, the result in Fig. 10b shows that the cumulative number of cases would be reduced for the higher immunity against mutant strain $(1-\delta_3)$ and higher value of mutation rate (ν_1). The result also shows that mutation rate has a negligible impact on cumulative cases when immunity against mutant strain is high. The result in Fig. 10c shows that the cumulative number of cases would be reduced for the higher vaccine efficacy against the mutant strain $(1-\delta_2)$ when mutation rate (ν_1) is high. The result also shows that

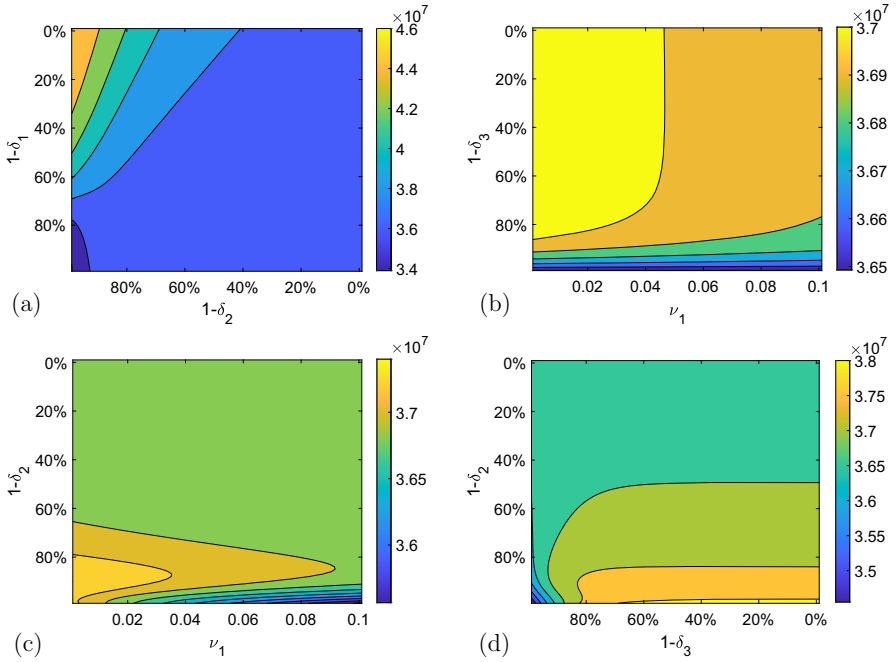

Fig. 10 Contour plots of the cumulative cases as a function of different parameters: **a** as a function of vaccine efficacy $(1-\delta_1)$ against native strain and vaccine efficacy $(1-\delta_2)$ against mutant strain; **b** as a function of immunity against mutant strain $(1-\delta_3)$ and mutation rate (ν_1); **c** as a function of vaccine efficacy $(1-\delta_2)$ against mutant strain and mutation rate (ν_1); **d** as a function of vaccine efficacy $(1-\delta_2)$ against mutant strain and immunity against mutant strain $(1-\delta_3)$. The baseline parameter values are used from Tables 2 and 3

cumulative cases would be higher for the higher values of $(1-\delta_2)$ and lower values of ν_1, which implies that the higher vaccine efficacy against mutant strain could not be able to control the disease. Figure 10d represents that the cumulative number of cases would be reduced only for higher immunity against mutant strain $(1-\delta_3)$. This result makes it wonder that cumulative cases would be higher even for the higher value of the vaccine efficacy against the mutant strain $(1-\delta_2)$ if there is a low value of immunity against mutant strain. This means there may exist an appropriate combination of these parameters to ensure fewer confirmed cases. Thus, it would be interesting to consider an optimal strategy for supplying vaccines to minimize the cumulative number of cases.

6.2 Impact of mutation rate on the dynamics of strains and infected population over time

The impact of mutation rate (ν_1) has been analyzed on the dynamics of strains and total infected population for COVID-19. We explicitly explore how the numbers of infected individuals I_1 and I_2 depend on the mutation parameter (ν_1). For this, we choose $\Lambda = 120000$, $\beta_2 = 3.9980e-08$ and other parametric values remain same as

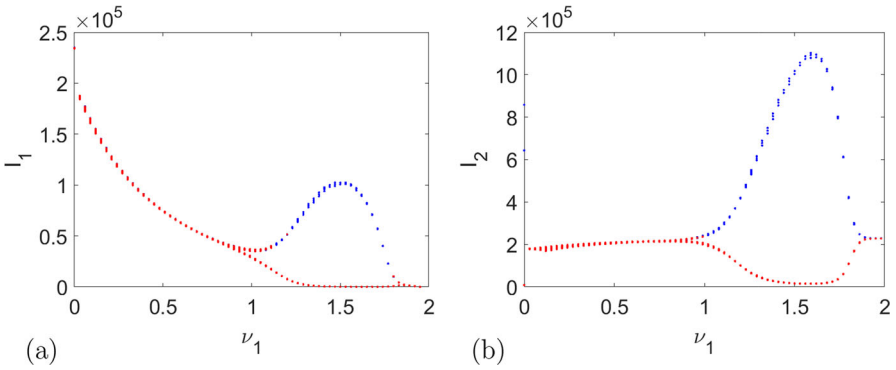

Fig. 11 Bifurcation diagram (endemic bubble) with respect to mutation rate (ν_1) for the fitted values of parameters given in Table 3. The blue color shows the upper limit of the limit cycle and red color shows the lower limit of the cycle (color figure online)

in Table 3. As shown in the bifurcation diagram (Fig. 11), for the range of mutation rate, $0 < \nu_1 \leq 0.9$, both strains persist in the environment, and system is asymptotically stable. For $0.9 < \nu_1 < 1.9$, the periodic oscillations (limit cycle) will appear, i.e. the disease outbreak will occur repeatedly. However, for a higher values of ν_1, i.e. for $\nu_1 \geq 1.9$, the periodic solutions disappear and the disease again becomes stable. This dynamical phenomenon has been illustrated in Fig. 12, for the values $\nu_1 = 0.5, 1.2$ and 2.0. Furthermore, we have plotted the total infected population $(E_1 + E_2 + I_1 + I_2)$ over time for different values of ν_1 in Fig. 13. This result gives a wondering dynamics over a long time. We can easily observe that if the mutation rate (ν_1) increases from 0.02 to 0.5, then the infected population persists at a lower level (blue and red curves). In addition, if the value of ν_1 is increased to 1.5, then the total infected population oscillates over time (yellow curve). If the value of ν_1 is further increased to 2, then the infected population persists at a much lower level (purple curve) over long time.

7 Sensitivity analysis

Our ultimate goal in developing a mathematical model of two strains with imperfect vaccine and mutation is to find the role of different parameters to control the disease. From the viewpoints of biological significance, R_0 plays a vital role in determining the severity (burden of disease), outcome and process of the infection. This section investigates how a percentage change in key parameters in the model (1) affects (changes) the basic reproduction number. If the basic reproduction number is brought below one, the disease infection will be eliminated. Even if the basic reproduction number cannot be brought below one, sensitivity analysis may help to determine which parameter, if acted upon, will bring the largest reduction in the basic reproduction numbers. Sensitivity indices measure the percentage change of a key quantity, such as the basic reproduction number, when a parameter value in that quantity is changed by a certain percentage. Sensitivity analysis is carried out on each parameter, which is utilized to recognize and check parameters responsible for impacting the basic reproductive num-

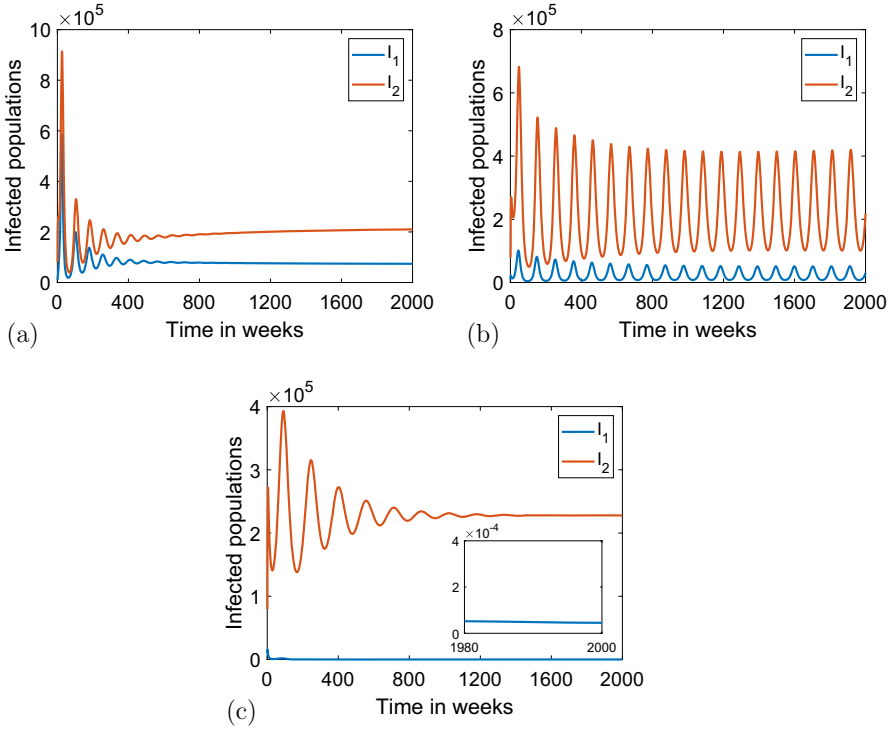

Fig. 12 Impact of mutation rate (ν_1) on the infected populations I_1 and I_2. **a** The asymptotically stable solutions I_1 and I_2 of system (1) for the parametric values in Table 3 and $\nu_1 = 0.5$. **b** The periodic solutions I_1 and I_2 of system (1) for $\nu_1 = 1.5$. **c** The asymptotically stable solutions I_1 and I_2 of system (1) for $\nu_1 = 2.0$

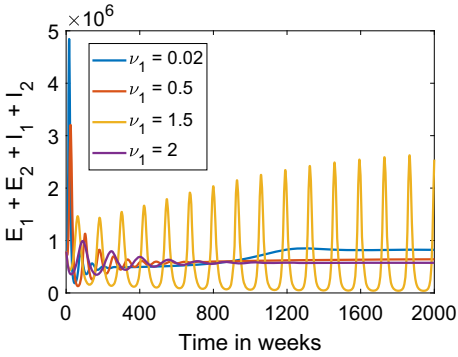

Fig. 13 Variation of the total infected population with respect to different values of ν_1

ber. The normalized sensitivity indices also called elasticity of a particular quantity Q with respect to the parameter p, is defined as follows (Martcheva 2014):

$$\epsilon_p^Q = \frac{\partial Q}{\partial p}\frac{p}{Q}. \tag{23}$$

Table 5 List of elasticities of R_1 and R_2

Parameters	Values of elasticities of R_1	Values of elasticities of R_2
Λ	1	1
β_1	1	–
β_2	–	1
a_1	0.00059	–
a_2	–	0.0009
γ	0.139	0.1077
μ	−1	−1
p	−0.14	−0.1085
δ_1	0.058	–
δ_2	–	0.0903
d_1	−0.013	–
d_2	–	−0.0138
α_1	−0.948	–
α_2	–	−0.985
ν_1	−0.0379	–

Elasticities can be positive or negative. A positive sign says that quantity Q increases with the increase in the parameter value of p, while a negative sign says that quantity Q decreases with the increase in the value of p.

We compute the elasticity indices for the basic reproduction numbers R_1 and R_2 given in Table 5. In Table 5, the parameters with positive sensitivity indices are those parameters that have a great influence on the development of the disease in the community if their values are increasing. This is because the basic reproduction number increases as the value of these parameter increases; that is, the average number of secondary cases of infection increases in the community. Also, all the parameters in which their indices are negative can curtail the infection in the community as their values increase while the others are left constant. As their values increase, the basic reproduction number decreases, which reduces the endemicity of the disease in the community.

It is evident from the values of elasticities that the reproduction numbers experience the highest impact with change to recruitment rate (Λ), transmission rates $((\beta_1)$ and $(\beta_2))$, natural death rate (μ), and recovery rates $((\alpha_1)$ and $(\alpha_2))$, where (Λ), (β_1), and (β_2) have positive sensitivities while μ, α_1, and α_2 have negative sensitivities.

We also perform global sensitivity analysis using the methodology of Latin Hypercube Sampling (LHS) and partial rank correlation coefficients (PRCCs) (Marino et al. 2008) to investigate the dependence of R_0 on the different parameters. From Fig. 14, we observe that recruitment rate (Λ), transmission rates (β_1, β_2), natural death rate (μ), and recovery rates (α_1, α_2) are the most sensitive parameters for R_0. To generate the LHS matrices, we assume that all the model parameters are uniformly distributed.

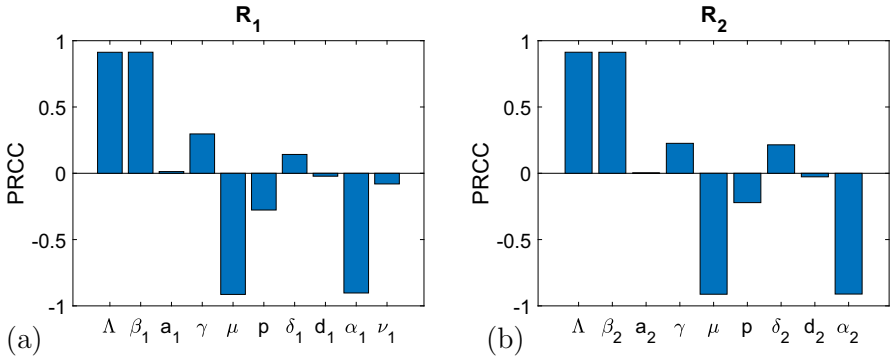

Fig. 14 PRCC sensitivity on R_0

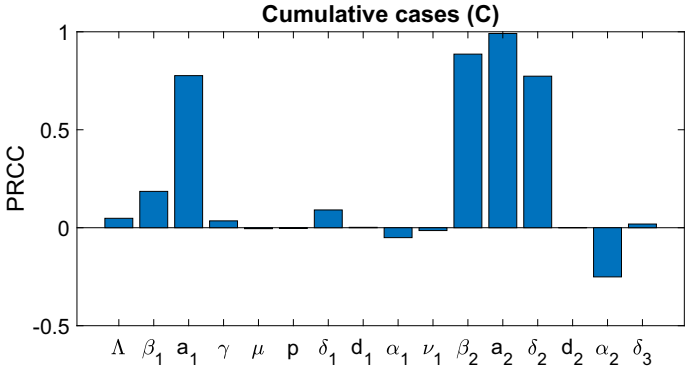

Fig. 15 PRCC sensitivity on cumulative cases (C)

Then using the baseline values from Tables 2 and 3, a total of 10,000 simulations per LHS run are carried out.

We also examine the impact of sensitivities of the parameters on the population sizes of cumulative cases (C) and deaths (D). From Fig. 15, we observe that a_1, β_2, a_2 and δ_2 are the most sensitive parameters to the cumulative cases, which means that the increasing value of these parameters increases the cumulative cases. This result implies that we should control these parameters to reduce the cumulative cases. From Fig. 16, we observe that $a_1, a_2, \beta_2, d_1, d_2,$ and α_2 are the most sensitive parameters to the cumulative deaths, where $\beta_2, a_1, a_2, d_1,$ and d_2 have positive sensitivities and α_2 has negative sensitivity, indicating that we should control the parameters $\beta_2, a_1, a_2, d_1, d_2$ and promote α_2 to reduce the cumulative deaths.

8 Discussion

The novel coronavirus has rapidly emerged as a disease COVID-19 and evolved as pandemics worldwide. The emergence of new variants of SARS-CoV-2 could complicate mitigation efforts. Reducing the transmission of the novel coronavirus pandemic

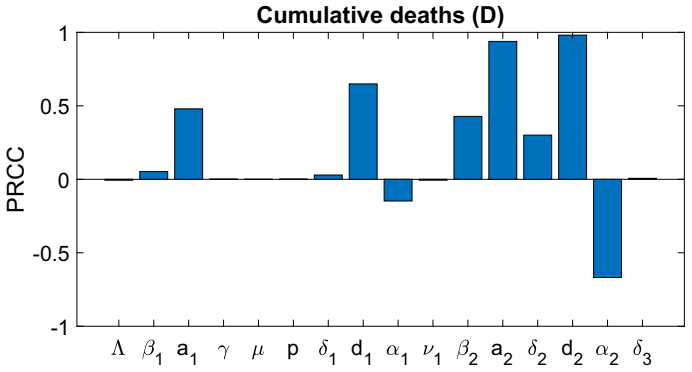

Fig. 16 PRCC sensitivity on cumulative deaths (D)

has been the massive responsibility of the intellects of every public health agencies, Govt. officials, and millions of populations worldwide. According to the World Health Organization (WHO) (World Health Organization 2021b), over 26 crore populations are infected with the COVID-19 as of December 4, 2021. Now the Govt. of different countries have been trying to give safeguards to the populations via vaccination. Since every vaccine is imperfect to the disease and the virus mutates over time, mathematical models may help to understand the dynamics of transmission and control of the novel coronavirus.

Taking care of the pandemic scenario, we proposed and analyzed an SEIR type multi-strain mathematical model (1) with imperfect vaccine and mutation. We also assumed that recovered individuals of native strain could become infected by the mutant strain, but they have some immunity against the mutant strain, and it has been modeled by multiplying a reduction coefficient to the transmission rate. The model we developed takes the form of a deterministic system of nonlinear differential equations. The model is rigorously analyzed to gain insights into its dynamical features. Theoretical and numerical analysis of the proposed system (1) have been carried out using stability theory. Positivity and boundedness of the solutions of system (1) have been studied, and the system (1) is well-posed. We found that the DFE (D^0) is globally asymptotically stable when $R_0 < 1$ in the presence of an imperfect vaccine, i.e., the native and mutant strains will be eliminated in the community whenever $R_0 < 1$. In other words, the imperfect vaccine against COVID-19 can lead to the eradication of the pandemic if it can bring (or maintain) R_0 to a value less than unity. Further, we analyzed the existence and stability of the mutant dominant equilibrium (D^2) by constructing a suitable Lyapunov function. Global stability of coexistence (endemic) equilibrium of both native and mutant strains has been investigated for the case $\nu_1 = 0$ and $\delta_3 = 0$, by constructing a suitable Lyapunov function. This result implies that if the mutation rate is zero and recovered individuals from native strain have 100% immunity against mutant strain, the disease persists in the environment at a certain level when $R_0 > 1$. Moreover, we investigated that system (1) undergoes a Hopf bifurcation. The transcritical bifurcation was also investigated for system (1) by using center manifold theory. By numerical simulation, we discovered that system (1) exhibits an interesting

dynamics called an endemic bubble, which means the system loses its stability for certain values of mutation rate (ν_1), and oscillations occur, and further for larger values of ν_1, the system regains its stability (refer the Fig. 5). The occurrence of Hopf bifurcation has also been ensured by varying the parameter δ_3 (Fig. 6), which implies that the disease will appear repeatedly for the higher values of δ_3.

We also computed an expression for herd immunity and a threshold value for the vaccination rate that suggest disease control implications. The mentioned necessary herd immunity (induced by vaccination) percentage may not be realistically achievable. Indeed, Dr. Anthony Fauci, a member of the US Presidential Task Force on COVID-19, said on June 29, 2020, that an imaginary anti-COVID-19 vaccine might not be helpful in attaining the requisite high immunity in the US if many people deny getting it Cable News Network (2020). One way to get around this requirement for high vaccine coverage to attain high immunity is to merge the vaccination program with other anti-COVID-19 intervention strategies, such as social distancing, the use of face masks in public, etc.

Furthermore, we parameterized the proposed mathematical model using the data of the COVID-19 pandemic in India, for assessing the potential community-wide impact of an imperfect vaccine against COVID-19 and mutation of the virus. Using the data of cumulative confirmed cases and deaths of COVID-19 in India from March 1, 2021 to September 27, 2021, and by employing the MCMC method to fit the model (1) with the data, the mean values, the standard deviation, and Geweke values of the unknown parameters were estimated.

We carried out numerical simulations to measure the population-level impact of the vaccine's efficacies. The results exhibited that the COVID-19 burden (as measured in terms of cumulative cases and deaths) decreases with increasing vaccine efficacies, as expected. We investigated how the cumulative number of cases varies with different values of vaccine efficacies against different strains, mutation rate, and immunity against the mutant strain in India. Our analysis showed what would happen if the vaccine efficacies against native and mutant strains were increased from their baseline values, as shown in Fig. 8a, b. The results showed that if the vaccine efficacy $(1 - \delta_1)$ was increased by its baseline value, then the cumulative cases would be decreased by November 29, 2021. Figure 8b demonstrated that if the vaccine efficacy against mutant strain $(1 - \delta_2)$ increased from its baseline value then cumulative cases would have decreased initially but not for longer time. We also assessed the impact of immunity against mutant strain $(1 - \delta_3)$ and observed that if the value of $(1 - \delta_3)$ is decreased from its baseline value, then the cumulative cases would be increased by November 29, 2021, shown in Fig. 8c. We also analyzed the impact of mutation rate on cumulative cases shows the reduction in cumulative cases with increasing mutation rate, depicted in Fig. 8d.

The cumulative number of deaths has also been varied with different values of vaccine's efficacies against different strains in Fig. 9. The results in Fig. 9a showed that if the vaccine efficacy against native strain $(1 - \delta_1)$ was increased from its baseline value, then the cumulative deaths would be decreased by November 29, 2021. Figure 9b demonstrated that if the vaccine efficacy against mutant strain increased from its baseline value, then cumulative deaths would be decreased. Our analysis also showed the combined impact of vaccine efficacies to both strains, which were increased to

20%, 40%, 60%, 80%, respectively, as shown in Fig. 10a. The result demonstrated that increasing the vaccine efficacy against the native strain is more influential in reducing the cumulative number of cases than the efficacy against mutant strain. We have shown in the contour plot (Fig. 10b) that there would be higher cumulative cases for the lower immunity against mutant strain even for the lower value of the mutation rate. There will be fewer cumulative cases if immunity against mutant strain is high. The contour plot (Fig. 10c) exhibited that cumulative cases would be high for the lower mutation rate and high vaccine efficacy against mutant strain. Furthermore, it has also been shown that immunity against mutant strain is more effective than vaccine efficacy against mutant strain in reducing the cumulative cases. This implies that there is a need to increase in the immunity against mutant strain $(1-\delta_3)$ to decrease the cumulative cases of COVID-19 in the presence of the mutation.

The endemic bubble phenomenon has been verified for COVID-19 by plotting the bifurcation diagram and periodic solutions for the fitted values from Table 3 in Figs. 11 and 12, respectively. These results imply that for a certain range of values of mutation rate (ν_1), the COVID-19 outbreaks will occur repeatedly. However, for the lower and higher enough values of ν_1, the disease remains stable in the environment. These dynamics represent a worse scenario for the mutation of the virus in the sense of the occurrence of periodic solutions. Furthermore, the total infected population has also been plotted for different values of mutation rate (ν_1) and a wondering dynamics has been observed. This result shows that for a high rate of mutation, the total infected population would be stable at a lower level over a long time. However, oscillation occurs for an intermediate range of mutation rate, implying that mutation may be worse in the sense of oscillation but better in the sense of stability at a lower infection level over a long time.

Furthermore, sensitivity analysis was performed to reveal the relative significance of the key epidemiological parameters of the system (1), which are $\Lambda, \beta_1, \beta_2, \alpha_1, \alpha_2$, because these parameters should be given priority to effectively control the disease. The PRCCs of the reproduction numbers (Fig. 14) provided that reducing $\Lambda, \beta_1, \beta_2$, which may be realized by strong control measures, such as lockdown, using face mask, travel restrictions, isolation of infected individuals, contact tracing, can significantly reduce R_0 and thus lower the transmission risk of COVID-19. The PRCCs of the cumulative cases and deaths suggest that the parameters a_1, a_2, β_2, and δ_2 should be controlled in order to reduce the cumulative cases; and a_1, a_2, β_2, d_1, and d_2 should be controlled in order to reduce the cumulative deaths.

We have to point out that the results in contour plots revealed an interesting problem, i.e., there may exist an optimal strategy of supplementing the vaccine with different efficacies, in order to ensure fewer cumulative cases and deaths, and the expenditure is economical, a topic for our future work. For preserving public health, it must focused on how the facility of medical resources availability affects the pandemic of COVID-19, which may be included in our model as future work. Formulating and analyzing the model with other non-pharmaceutical interventions (Xue et al. 2022) with vaccination will be more helpful to control the spread of multi-strain disease. For instance, Iboi et al. (2020) proposed a dynamical model to assess the impact of vaccine strategy with other public health intervention strategies; in particular, the authors assessed the impact of vaccine efficacy combined with mask efficacy concerning COVID-19 in the

US. Their results confirmed that the elimination of COVID-19 is more feasible if the vaccine program is combined with other interventions. We focused on the situation in India, but the model may be extended to describe the efficacies of vaccines against different strains with mutation rates and developed immunity against other mutant variants of SARS-CoV-2 in other countries.

Acknowledgements The research work of Sarita Bugalia is supported by the Council of Scientific & Industrial Research (CSIR), India [File No. 09/1131(0025)/2018-EMR-I]. The research work of Jai Prakash Tripathi is supported by the Science and Engineering Research Board (SERB), India [File No. ECR/2017/002786] and [File No. MTR/2022/001028]. We are highly thankful to all the anonymous reviewers and editor for their insightful comments and suggestions, which helped us to improve the manuscript considerably.

Appendix A

$$
\begin{aligned}
l_1 &= -(a_{11}+b_{12}+c_{13}+d_{13}+e_{12}+f_{13}+g_{13}),\\
l_2 &= -a_{12}b_{11}+c_{13}d_{13}+c_{13}e_{12}-c_{14}e_{11}+d_{13}e_{12}-d_{14}f_{11}+(c_{13}+d_{13}+e_{12})f_{13}\\
&\quad+g_{13}(c_{13}+d_{13}+e_{12}+f_{13})+b_{12}(c_{13}+d_{13}+e_{12}+f_{13}+g_{13})\\
&\quad+a_{11}(b_{12}+c_{13}+d_{13}+e_{12}+f_{13}+g_{13}),\\
l_3 &= a_{11}(-b_{12}(c_{13}+d_{13}+e_{12}+f_{13}+g_{13})-c_{13}(d_{13}+e_{12}+f_{13}+g_{13})+c_{14}e_{11}\\
&\quad-g_{13}(d_{13}+e_{12}+f_{13})-d_{13}e_{12}-d_{13}f_{13}+d_{14}f_{11}-e_{12}f_{13})\\
&\quad+a_{12}b_{11}(c_{13}+d_{13}+e_{12}+f_{13}+g_{13})-g_{13}(b_{12}(c_{13}+d_{13}+e_{12}+f_{13})\\
&\quad+c_{13}(d_{13}+e_{12}+f_{13})-c_{14}e_{11}+f_{13}(d_{13}+e_{12})+d_{13}e_{12}-d_{14}f_{11})\\
&\quad-e_{11}(a_{13}c_{11}+b_{13}c_{12})-c_{13}d_{13}e_{12}+c_{13}d_{14}f_{11}-c_{13}d_{13}f_{13}-c_{13}e_{12}f_{13}\\
&\quad-f_{11}(a_{14}d_{11}+b_{14}d_{12})+d_{14}e_{12}f_{11}-d_{13}e_{12}f_{13}+c_{14}e_{11}(d_{13}+f_{13})-d_{15}f_{11}g_{12}\\
&\quad-b_{12}(c_{13}(d_{13}+e_{12}+f_{13})-c_{14}e_{11}+f_{13}(d_{13}+e_{12})+d_{13}e_{12}-d_{14}f_{11}),
\end{aligned}
$$

$$
\begin{aligned}
l_4 &= a_{13}e_{11}(c_{11}(b_{12}+d_{13})-b_{11}c_{12})+d_{13}(b_{12}c_{13}e_{12}-b_{12}c_{14}e_{11}+b_{13}c_{12}e_{11})\\
&\quad+f_{11}(a_{14}(d_{11}(b_{12}+c_{13}+e_{12})-b_{11}d_{12})-d_{14}(e_{12}(b_{12}+c_{13})+b_{12}c_{13}-c_{14}e_{11})\\
&\quad+b_{14}d_{12}(c_{13}+e_{12}))-a_{12}(b_{11}(c_{13}(d_{13}+e_{12})-c_{14}e_{11}+d_{13}e_{12}\\
&\quad-d_{14}f_{11})+b_{13}c_{11}e_{11}\\
&\quad+b_{14}d_{11}f_{11})-e_{11}f_{12}(a_{14}c_{11}+b_{14}c_{12})\\
&\quad+b_{12}c_{13}d_{13}f_{13}+f_{13}(a_{13}c_{11}e_{11}\\
&\quad+e_{12}(d_{13}(b_{12}+c_{13})+b_{12}c_{13})-c_{14}e_{11}(b_{12}+d_{13})+b_{13}c_{12}e_{11})\\
&\quad-a_{12}b_{11}f_{13}(c_{13}+d_{13}+e_{12})+d_{15}f_{11}g_{12}(b_{12}+c_{13}+e_{12})-a_{12}b_{11}g_{13}(c_{13}\\
&\quad+d_{13}+e_{12}+f_{13})+g_{13}(a_{13}c_{11}e_{11}+a_{14}d_{11}f_{11}+b_{12}(c_{13}(d_{13}+e_{12}+f_{13})\\
&\quad-c_{14}e_{11}+f_{13}(d_{13}+e_{12})+d_{13}e_{12}-d_{14}f_{11})+b_{13}c_{12}e_{11}+b_{14}d_{12}f_{11}\\
&\quad+c_{13}d_{13}e_{12}+c_{13}d_{13}f_{13}-c_{13}d_{14}f_{11}+c_{13}e_{12}f_{13}-c_{14}e_{11}(d_{13}+f_{13})\\
&\quad+d_{13}e_{12}f_{13}-d_{14}e_{12}f_{11})+a_{11}(b_{13}c_{12}e_{11}+b_{14}d_{12}f_{11}+c_{13}(f_{13}(d_{13}+e_{12})\\
&\quad+d_{13}e_{12}-d_{14}f_{11})+d_{13}e_{12}f_{13}-d_{14}e_{12}f_{11}+d_{15}f_{11}g_{12})+a_{11}(b_{12}(c_{13}(d_{13}
\end{aligned}
$$

$$
\begin{aligned}
&+ e_{12} + f_{13} + g_{13}) - c_{14}e_{11} + d_{13}(e_{12} + f_{13} + g_{13}) - d_{14}f_{11} + g_{13}(e_{12} + f_{13})\\
&+ e_{12}f_{13}) + g_{13}(c_{13}(d_{13} + e_{12} + f_{13}) + d_{13}(e_{12} + f_{13}) - d_{14}f_{11} + e_{12}f_{13})\\
&- c_{14}e_{11}(d_{13} + f_{13} + g_{13})),
\end{aligned}
$$

$$
\begin{aligned}
l_5 = {} & a_{12}(b_{11}(g_{13}(c_{13}(d_{13} + e_{12} + f_{13}) + f_{13}(d_{13} + e_{12}) + d_{13}e_{12} - d_{14}f_{11}) + c_{13}d_{13}e_{12}\\
&+ c_{13}d_{13}f_{13} - c_{13}d_{14}f_{11} + c_{13}e_{12}f_{13} - c_{14}e_{11}(d_{13} + f_{13} + g_{13}) + d_{13}e_{12}f_{13}\\
&- d_{14}e_{12}f_{11} + d_{15}f_{11}g_{12}) + b_{13}c_{11}e_{11}(d_{13} + f_{13} + g_{13})\\
&+ b_{14}(d_{11}f_{11}(c_{13} + e_{12} + g_{13})\\
&- c_{11}e_{11}f_{12})) - a_{13}e_{11}(-b_{11}c_{12}(d_{13} + f_{13} + g_{13}) + b_{12}c_{11}(d_{13} + f_{13} + g_{13})\\
&+ c_{11}(g_{13}(d_{13} + f_{13}) + d_{13}f_{13} - d_{14}f_{11})) - g_{13}(f_{11}(a_{14}(d_{11}(c_{13} + e_{12}) - b_{11}d_{12})\\
&+ b_{14}d_{12}(c_{13} + e_{12}) - c_{13}d_{14}e_{12} + c_{14}d_{14}e_{11}) - b_{12}(-a_{14}d_{11}f_{11} - c_{13}d_{13}e_{12}\\
&+ d_{14}f_{11}(c_{13} + e_{12}) + c_{14}d_{13}e_{11}) - e_{11}f_{12}(a_{14}c_{11} + b_{14}c_{12}) + b_{13}c_{12}d_{13}e_{11}\\
&+ f_{13}(b_{12}(c_{13}(d_{13} + e_{12}) - c_{14}e_{11} + d_{13}e_{12}) + b_{13}c_{12}e_{11} + c_{13}d_{13}e_{12} - c_{14}d_{13}e_{11})\\
&+ a_{11}(b_{12}(c_{13}(d_{13} + e_{12} + f_{13}) - c_{14}e_{11} + f_{13}(d_{13} + e_{12}) + d_{13}e_{12} - d_{14}f_{11})\\
&+ b_{13}c_{12}e_{11} + b_{14}d_{12}f_{11} + c_{13}d_{13}e_{12} + c_{13}d_{13}f_{13} - c_{13}d_{14}f_{11} + c_{13}e_{12}f_{13}\\
&- c_{14}e_{11}(d_{13} + f_{13}) + d_{13}e_{12}f_{13} - d_{14}e_{12}f_{11})) + a_{14}e_{11}f_{12}(c_{11}(b_{12}\\
&+ d_{13}) - b_{11}c_{12})\\
&+ a_{14}f_{11}(b_{11}d_{12}(c_{13} + e_{12}) - b_{12}d_{11}(c_{13} + e_{12}) - c_{13}d_{11}e_{12} + c_{14}d_{11}e_{11})\\
&- d_{15}f_{11}g_{12}(b_{12}(c_{13} + e_{12}) + c_{13}e_{12} - c_{14}e_{11}) + b_{14}c_{12}d_{13}e_{11}f_{12}\\
&+ f_{11}(d_{14}(b_{12}c_{13}e_{12}\\
&- b_{12}c_{14}e_{11} + b_{13}c_{12}e_{11}) + b_{14}d_{12}(c_{14}e_{11} - c_{13}e_{12})) - d_{13}f_{13}(b_{12}c_{13}e_{12}\\
&- b_{12}c_{14}e_{11} + b_{13}c_{12}e_{11}) + a_{11}(-f_{13}(b_{12}(c_{13}(d_{13} + e_{12}) - c_{14}e_{11} + d_{13}e_{12})\\
&+ b_{13}c_{12}e_{11} + c_{13}d_{13}e_{12}\\
&- c_{14}d_{13}e_{11}) - b_{12}c_{13}d_{13}e_{12} + b_{12}c_{13}d_{14}f_{11} - d_{15}f_{11}g_{12}(b_{12}\\
&+ c_{13} + e_{12}) + b_{12}c_{14}d_{13}e_{11}\\
&+ b_{12}d_{14}e_{12}f_{11} - b_{13}c_{12}d_{13}e_{11} + b_{14}c_{12}e_{11}f_{12} - b_{14}c_{13}d_{12}f_{11}\\
&- b_{14}d_{12}e_{12}f_{11}\\
&+ c_{13}d_{14}e_{12}f_{11} - c_{14}d_{14}e_{11}f_{11}),
\end{aligned}
$$

$$
\begin{aligned}
l_6 = {} & a_{13}e_{11}(-g_{13}(b_{11}c_{12}(d_{13} + f_{13}) - c_{11}d_{13}f_{13} + c_{11}d_{14}f_{11})\\
&- b_{11}c_{12}d_{13}f_{13} + b_{11}c_{12}d_{14}f_{11}\\
&+ b_{12}c_{11}(g_{13}(d_{13} + f_{13}) + d_{13}f_{13} - d_{14}f_{11}) + b_{14}f_{11}(c_{11}d_{12} - c_{12}d_{11})\\
&+ c_{11}d_{15}f_{11}g_{12})\\
&+ a_{14}(b_{11}c_{12}d_{13}e_{11}f_{12} - b_{11}c_{13}d_{12}e_{12}f_{11} + b_{11}c_{14}d_{12}e_{11}f_{11} - b_{12}(c_{11}d_{13}e_{11}f_{12}\\
&- c_{13}d_{11}e_{12}f_{11} + c_{14}d_{11}e_{11}f_{11}) + b_{13}e_{11}f_{11}(c_{12}d_{11} - c_{11}d_{12}) - c_{11}d_{15}e_{11}f_{11}g_{11}\\
&+ g_{13}(f_{11}(-b_{11}d_{12}(c_{13} + e_{12}) + b_{12}d_{11}(c_{13} + e_{12}) + c_{13}d_{11}e_{12} - c_{14}d_{11}e_{11})\\
&- e_{11}f_{12}(c_{11}(b_{12} + d_{13}) - b_{11}c_{12}))) - g_{13}(a_{11}(b_{12}d_{13}(c_{14}e_{11} - c_{13}e_{12})\\
&+ b_{12}d_{14}f_{11}(c_{13} + e_{12}) - b_{13}c_{12}d_{13}e_{11} + b_{14}c_{12}e_{11}f_{12} - f_{11}(b_{14}d_{12}(c_{13} + e_{12})
\end{aligned}
$$

$$
\begin{aligned}
&- c_{13}d_{14}e_{12} + c_{14}d_{14}e_{11})) + d_{14}f_{11}(b_{12}c_{13}e_{12} - b_{12}c_{14}e_{11} + b_{13}c_{12}e_{11})\\
&+ b_{14}(c_{12}d_{13}e_{11}f_{12} - c_{13}d_{12}e_{12}f_{11} + c_{14}d_{12}e_{11}f_{11})\\
&+ a_{12}(b_{11}(c_{13}(f_{13}(d_{13} + e_{12})\\
&+ d_{13}e_{12} - d_{14}f_{11}) - c_{14}e_{11}(d_{13} + f_{13}) + d_{13}e_{12}f_{13} - d_{14}e_{12}f_{11})\\
&+ b_{13}c_{11}e_{11}(d_{13} + f_{13})\\
&- b_{14}c_{11}e_{11}f_{12} + b_{14}d_{11}f_{11}(c_{13} + e_{12})) - f_{13}(a_{11}(b_{12}(e_{12}(c_{13} + d_{13})\\
&+ c_{13}d_{13} - c_{14}e_{11})\\
&+ b_{13}c_{12}e_{11} + c_{13}d_{13}e_{12} - c_{14}d_{13}e_{11}) + d_{13}(b_{12}c_{13}e_{12}\\
&- b_{12}c_{14}e_{11} + b_{13}c_{12}e_{11})))\\
&+ a_{11}(-(d_{14}f_{11} - d_{13}f_{13})(b_{12}c_{13}e_{12} - b_{12}c_{14}e_{11} + b_{13}c_{12}e_{11})\\
&+ d_{15}f_{11}g_{12}(e_{12}(b_{12} + c_{13})\\
&+ b_{12}c_{13} - c_{14}e_{11}) - b_{14}(c_{12}d_{13}e_{11}f_{12} - c_{13}d_{12}e_{12}f_{11}\\
&+ c_{14}d_{12}e_{11}f_{11})) + a_{12}((d_{14}f_{11}\\
&- d_{13}f_{13})(b_{11}c_{13}e_{12} - b_{11}c_{14}e_{11} + b_{13}c_{11}e_{11}) - b_{11}d_{15}f_{11}g_{12}(c_{13} + e_{12})\\
&+ b_{14}(c_{11}d_{13}e_{11}f_{12} - c_{13}d_{11}e_{12}f_{11} + c_{14}d_{11}e_{11}f_{11}))\\
&+ d_{15}f_{11}(g_{12}(b_{12}c_{13}e_{12} - b_{12}c_{14}e_{11}\\
&+ b_{13}c_{12}e_{11}) - b_{14}c_{12}e_{11}g_{11}),
\end{aligned}
$$

$$
\begin{aligned}
l_7 =&a_{14}d_{15}e_{11}f_{11}g_{11}(b_{12}c_{11} - b_{11}c_{12}) + g_{13}(a_{11}((d_{14}f_{11} - d_{13}f_{13})\\
&(b_{12}c_{13}e_{12} - b_{12}c_{14}e_{11}\\
&+ b_{13}c_{12}e_{11}) + b_{14}(c_{12}d_{13}e_{11}f_{12} - c_{13}d_{12}e_{12}f_{11} + c_{14}d_{12}e_{11}f_{11}))\\
&- a_{12}(d_{14}f_{11}(b_{11}c_{13}e_{12}\\
&- b_{11}c_{14}e_{11} + b_{13}c_{11}e_{11}) + b_{14}(c_{11}d_{13}e_{11}f_{12} - c_{13}d_{11}e_{12}f_{11} + c_{14}d_{11}e_{11}f_{11}))\\
&+ a_{12}d_{13}f_{13}(b_{11}c_{13}e_{12} - b_{11}c_{14}e_{11} + b_{13}c_{11}e_{11}) + a_{13}e_{11}((b_{12}c_{11} - b_{11}c_{12})(d_{14}f_{11}\\
&- d_{13}f_{13}) + b_{14}f_{11}(c_{12}d_{11} - c_{11}d_{12}))) + d_{15}f_{11}(g_{12}(e_{11}(a_{11}b_{12}c_{14} - a_{11}b_{13}c_{12}\\
&- a_{12}b_{11}c_{14} + a_{12}b_{13}c_{11} + a_{13}b_{11}c_{12} - a_{13}b_{12}c_{11}) + c_{13}e_{12}(a_{12}b_{11} - a_{11}b_{12}))\\
&+ b_{14}e_{11}g_{11}(a_{11}c_{12} - a_{12}c_{11})) + a_{14}g_{13}(d_{13}e_{11}f_{12}(b_{12}c_{11} - b_{11}c_{12}) + f_{11}(b_{12}d_{11}\\
&- b_{11}d_{12})(c_{14}e_{11} - c_{13}e_{12}) + b_{13}e_{11}f_{11}(c_{11}d_{12} - c_{12}d_{11})).
\end{aligned}
$$

$$
\begin{aligned}
&a_{11} = -\beta_1 I_1^* - \beta_2 I_2^* - (\mu + p), \quad a_{12} = \gamma, \quad a_{13} = -\beta_1 S^*, \quad a_{14} = -\beta_2 S^*,\\
&b_{11} = p, \quad b_{12} = -\delta_1\beta_1 I_1^* - \delta_2\beta_2 I_2^* - (\mu + \gamma), \quad b_{13} = -\delta_1\beta_1 V^*,\\
&b_{14} = -\delta_2\beta_2 V^*, \quad c_{11} = \beta_1 I_1^*, \quad c_{12} = \delta_1\beta_1 I_1^*, \quad c_{13} = -(a_1 + \mu),\\
&c_{14} = \beta_1(S^* + \delta_1 V^*), \quad d_{11} = \beta_2 I_2^*, \quad d_{12} = \delta_2\beta_2 I_2^*, \quad d_{13} = -(a_2 + \mu),\\
&d_{14} = \beta_2(S^* + \delta_2 V^*) + \delta_3\beta_2 R_1^*, \quad d_{15} = \delta_3\beta_2 I_2^*, \quad e_{11} = a_1,\\
&e_{12} = -(\alpha_2 + \mu + d_1 + \nu_1), \quad f_{11} = a_2, \quad f_{12} = \nu_1, \quad f_{13} = -(\alpha_2 + \mu + d_2),\\
&g_{11} = \alpha_1, \quad g_{12} = -\delta_3\beta_2 R_1^*, \quad g_{13} = -(\delta_3\beta_2 I_2^* + \mu).
\end{aligned}
$$

References

Ahmed SE (2008). Markov chain monte carlo: Stochastic simulation for bayesian inference. https://doi.org/10.1198/tech.2008.s542

Alexander ME, Bowman C, Moghadas SM, Summers R, Gumel AB, Sahai BM (2004) A vaccination model for transmission dynamics of influenza. SIAM J Appl Dyn Syst 3(4):503–524. https://doi.org/10.1137/030600370

Anderson RM (1992) The concept of herd immunity and the design of community-based immunization programmes. Vaccine 10:928e935. https://doi.org/10.1016/0264-410X(92)90327-G

Anderson RM, May RM (1985) Vaccination and herd immunity to infectious diseases. Nature 318:323e329. https://doi.org/10.1038/318323a0

Arino J, McCluskey CC, van den Driessche P (2003) Global results for an epidemic model with vaccination that exhibits backward bifurcation. SIAM J Appl Math 64(1):260–276. https://doi.org/10.1137/S0036139902413829

Arruda EF, Pastore DH, Dias CM, Das SS (2021) Modelling and optimal control of multi strain epidemics, with application to COVID-19. https://doi.org/10.1371/journal.pone.0257512; arXiv preprint arXiv:2101:08137

Bajiya VP, Bugalia S, Tripathi JP (2020) Mathematical modeling of COVID-19: impact of non-pharmaceutical interventions in India. Chaos: Interdiscip J Nonlinear Sci 30(11):113143. https://doi.org/10.1063/5.0021353

Bonhoeffer S, Nowak MA (1994) Mutation and the evolution of virulence. Proc R Soc Lond Ser B: Biol Sci 258(1352):133–140. https://doi.org/10.1098/rspb.1994.0153

Bugalia S, Bajiya VP, Tripathi JP, Li MT, Sun GQ (2020) Mathematical modeling of COVID-19 transmission: the roles of intervention strategies and lockdown. Math Biosci Eng 17(5):5961–5986. https://doi.org/10.3934/mbe.2020318

Bugalia S, Tripathi JP, Wang H (2021) Mathematical modeling of intervention and low medical resource availability with delays: Applications to COVID-19 outbreaks in Spain and Italy. Math Biosci Eng 18(5):5865–5920. https://doi.org/10.3934/mbe.2021295

Bugalia S, Tripathi JP, Wang H (2023) Estimating the time-dependent effective reproduction number and vaccination rate for COVID-19 in the USA and India. Math Biosci Eng 20(3):4673–4689. https://doi.org/10.3934/mbe.2023216

Bussiness Insider (2021) https://tinyurl.com/6q3g47b8. Accessed 2 Nov 2021

Butler G, Freedman HI, Waltman P (1986) Uniformly persistent systems. Proc Am Math Soc 96(3):425–430. https://doi.org/10.2307/2046588

Cable News Network (2020) Fauci says covid-19 vaccine may not get us to herd immunity if too many people refuse to get it, CNN. https://edition.cnn.com/2020/06/28/health/fauci-coronavirus-vaccine-contact-tracing-aspen/index.html. Accessed 10 Sept 2021

Cai L, Xiang J, Li X, Lashari AA (2012) A two-strain epidemic model with mutant strain and vaccination. J Appl Math Comput 40(1):125–142. https://doi.org/10.1007/s12190-012-0580-x

Cai LM, Li Z, Song X (2018) Global analysis of an epidemic model with vaccination. J Appl Math Comput 57(1):605–628. https://doi.org/10.1007/s12190-017-1124-1

Castillo-Chavez C, Blower S, Van den Driessche P, Kirschner D, Yakubu AA, (eds) (2002) Mathematical approaches for emerging and reemerging infectious diseases: models, methods, and theory. Springer, Berlin. https://doi.org/10.1007/978-1-4613-0065-6

Castillo-Chavez C, Feng Z, Huang W (2002) On the computation of R_0 and its role in global stability. IMA Vol Math Appl 125:229–250

Castillo-Chavez C, Song B (2004) Dynamical models of tuberculosis and their applications. Math Biosci Eng 1(2):361. https://doi.org/10.3934/mbe.2004.1.361

Centers for Disease Control and Prevention (CDC) (2021a). https://www.cdc.gov/coronavirus/2019-ncov/variants/variant-classifications.html. Accessed 13 Oct 2021

Centers for Disease Control and Prevention (CDC) (2021b). https://www.cdc.gov/coronavirus/2019-ncov/your-health/reinfection.html. Accessed 13 Oct 2021

Chowdhury MM, Islam MR, Hossain MS, Tabassum N, Peace A (2022) Incorporating the mutational landscape of SARS-COV-2 variants and case-dependent vaccination rates into epidemic models. Infect Disease Model 7(2):75–82. https://doi.org/10.1016/j.idm.2022.02.003

Deng X, Garcia-Knight MA, Khalid MM, Servellita V, Wang C, Morris MK, Sotomayor-González A, Glasner DR, Reyes KR, Gliwa AS, Reddy NP (2021) Transmission, infectivity, and neutralization of a spike L452R SARS-CoV-2 variant. Cell. https://doi.org/10.1016/j.cell.2021.04.025

Diekmann O, Heesterbeek JA, Roberts MG (2010) The construction of next-generation matrices for compartmental epidemic models. J R Soc Interface 7(47):873–885. https://doi.org/10.1098/rsif.2009.0386

Duong BV, Larpruenrudee P, Fang T, Hossain SI, Saha SC, Gu Y, Islam MS (2022) Is the SARS CoV-2 omicron variant deadlier and more transmissible than delta variant? Int J Environ Res Public Health 19(8):4586. https://doi.org/10.3390/ijerph19084586

Elbasha EH, Gumel AB (2021) Vaccination and herd immunity thresholds in heterogeneous populations. J Math Biol. https://doi.org/10.1007/s00285-021-01686-z

Eletreby R, Zhuang Y, Carley KM, Yağan O, Poor HV (2020) The effects of evolutionary adaptations on spreading processes in complex networks. Proc Natl Acad Sci 117(11):5664–5670. https://doi.org/10.1073/pnas.1918529117

Eron JJ, Vernazza PL, Johnston DM, Seillier-Moiseiwitsch F, Alcorn TM, Fiscus SA, Cohen MS (1998) Resistance of HIV-1 to antiretroviral agents in blood and seminal plasma: implications for transmission. AIDS 12(15):F181–F189. https://doi.org/10.1097/00002030-199815000-00003

Freedman HI, Waltman P (1985) Persistence in a model of three competitive populations. Math Biosci 73(1):89–101. https://doi.org/10.1016/0025-5564(85)90078-1

Friedman TL (2020) Is Sweden doing it right? New York Times. https://www.nytimes.com/2020/04/28/opinion/coronavirus-sweden.html. Accessed 3 Oct 2021

Fudolig M, Howard R (2020) The local stability of a modified multi-strain SIR model for emerging viral strains. PLoS ONE 15(12):e0243408. https://doi.org/10.1371/journal.pone.0243408

Gonzalez-Parra G, Martínez-Rodríguez D, Villanueva-Micó RJ (2021) Impact of a new SARS-CoV-2 variant on the population: A mathematical modeling approach. Math Comput Appl 26(2):25. https://doi.org/10.3390/mca26020025

Gukenheimer J, Holmes P (1983) Nonlinear oscillations, Dynamical Systems, and Bifurcation of Vector Fields. Springer, New York. https://doi.org/10.1007/978-1-4612-1140-2

Gumel AB, McCluskey CC, Watmough J (2006) An SVEIR model for assessing potential impact of an imperfect anti-SARS vaccine. Math Biosci Eng 3(3):485. https://doi.org/10.3934/mbe.2006.3.485

Gupta S, Ferguson NM, Anderson RM (1997) Vaccination and the population structure of antigenically diverse pathogens that exchange genetic material. Proc R Soc Lond B 264(1387):1435–1443. https://doi.org/10.1098/rspb.1997.0200

Haario H, Laine M, Mira A, Saksman E (2006) DRAM: efficient adaptive MCMC. Stat Comput 16(4):339–354. https://doi.org/10.1007/s11222-006-9438-0

Haario H, Saksman E, Tamminen J (2001) An adaptive Metropolis algorithm. Bernoulli 7(2):223–242. https://doi.org/10.2307/3318737

Health, The Sciences (2021) https://science.thewire.in/the-sciences/covid-19-reinfection-hong-kong-man-immunity/. Accessed 10 Nov 2021

Hethcote HW (2000) The mathematics of infectious diseases. SIAM Rev Soc Ind Appl Math 42(4):599–653. https://doi.org/10.1137/S0036144500371907

How Dangerous Is the Delta Variant (B.1.617.2)? (2023) American society of microbiology. https://asm.org/Articles/2021/July/How-Dangerous-is-the-Delta-Variant-B-1-617-2. Accessed 20 June 2023

Iboi EA, Ngonghala CN, Gumel AB (2020) Will an imperfect vaccine curtail the COVID-19 pandemic in the US? Infect Disease Model 5:510–524. https://doi.org/10.1016/j.idm.2020.07.006

Iboi EA, Sharomi OO, Ngonghala CN, Gumel AB (2020) Mathematical modeling and analysis of COVID-19 pandemic in Nigeria. Math Biosci Eng 17(6):7192–7220. https://doi.org/10.3934/mbe.2020369

Iwami S, Takeuchi Y, Liu X (2007) Avian-human influenza epidemic model. Math Biosci 207(1):1–25. https://doi.org/10.1016/j.mbs.2006.08.001

Johns Hopkins Medicine (2021) https://www.hopkinsmedicine.org/health/conditions-and-diseases/coronavirus/a-new-strain-of-coronavirus-what-youshould-know. Accessed 17 Sept 2021

Kermack WO, McKendrick AG (1927) A contribution to the mathematical theory of epidemics. Proc R Soc Lond Ser A Contain Pap Math Phys Charact 115(772):700–721. https://doi.org/10.1098/rspa.1927.0118

Khyar O, Allali K (2020) Global dynamics of a multi-strain SEIR epidemic model with general incidence rates: application to COVID-19 pandemic. Nonlinear Dyn 102(1):489–509. https://doi.org/10.1007/s11071-020-05929-4

Korber B, Fischer WM, Gnanakaran S, Yoon H, Theiler J, Abfalterer W, Hengartner N, Giorgi EE, Bhattacharya T, Foley B, Hastie KM (2020) Tracking changes in SARS-CoV-2 Spike: evidence that D614G increases infectivity of the COVID-19 virus. Cell 182(4):812–827. https://doi.org/10.1016/j.cell.2020.06.043

LaSalle JP (1976) The stability of dynamical systems. Soc Ind Appl Math. https://doi.org/10.1137/1.9781611970432

Lauer SA, Grantz KH, Bi Q, Jones FK, Zheng Q, Meredith HR, Azman AS, Reich NG, Lessler J (2020) The incubation period of coronavirus disease 2019 (COVID-19) from publicly reported confirmed cases: estimation and application. Ann Intern Med 172(9):577–582. https://doi.org/10.7326/M20-0504

Lemieux JE, Li JZ (2021) Uncovering ways that emerging SARS-CoV-2 lineages may increase transmissibility. J Infect Dis 223(10):1663–1665. https://doi.org/10.1093/infdis/jiab083

Li J, Zhou Y, Ma Z, Hyman JM (2004) Epidemiological models for mutating pathogens. SIAM J Appl Math 65(1):1–23. https://doi.org/10.1137/S0036139903430185

Liu L, Ren X, Liu X (2018) Dynamical behaviors of an influenza epidemic model with virus mutation. J Biol Syst 26(03):455–472. https://doi.org/10.1142/S0218339018500201

Liu M, Liz E, Rost G (2015) Endemic bubbles generated by delayed behavioral response: global stability and bifurcation switches in an SIS model. SIAM J Appl Math 75(1):75–91. https://doi.org/10.1137/140972652

Liu WM (1994) Criterion of Hopf bifurcations without using eigenvalues. J Math Anal Appl 182(1):250–256. https://doi.org/10.1006/jmaa.1994.1079

Liu X, Takeuchi Y, Iwami S (2008) SVIR epidemic models with vaccination strategies. J Theor Biol 253(1):1–11. https://doi.org/10.1016/j.jtbi.2007.10.014

MacIntyre CR, Costantino V, Trent MJ (2021) Modelling of COVID-19 vaccination strategies and herd immunity, in scenarios of limited and full vaccine supply in NSW. Vaccine, Australia. https://doi.org/10.1016/j.vaccine.2021.04.042

Marino S, Hogue IB, Ray CJ, Kirschner DE (2008) A methodology for performing global uncertainty and sensitivity analysis in systems biology. J Theor Biol 254(1):178–196. https://doi.org/10.1016/j.jtbi.2008.04.011

Martcheva M (2015) An introduction to mathematical epidemiology. Springer, New York. https://doi.org/10.1007/978-1-4899-7612-3

Martcheva M, Iannelli M, Li XZ (2007) Subthreshold coexistence of strains: the impact of vaccination and mutation. Math Biosci Eng 4(2):287. https://doi.org/10.3934/mbe.2007.4.287

May RM, Nowak MA (1995) Coinfection and the evolution of parasite virulence. Proc R Soc Lond B 261(1361):209–215. https://doi.org/10.1098/rspb.1995.0138

May RM, Nowak MA (1994) Superinfection, metapopulation dynamics, and the evolution of diversity. J Theor Biol 170(1):95–114. https://doi.org/10.1006/jtbi.1994.1171

McLean AR (1995) Vaccination, evolution and changes in the efficacy of vaccines: a theoretical framework. Proc R Soc Lond B 261(1362):389–393. https://doi.org/10.1098/rspb.1995.0164

Ministry of Health and Family Welfare, Government of India (2021). https://www.mohfw.gov.in/covid_vaccination/vaccination/faqs.html#what-to-expect-before-vaccination-2. Accessed 16 Oct 2021

Nature news (2021) https://www.nature.com/articles/d41586-021-01059-y. Accessed 18 Oct 2021

Olliaro P, Torreele E, Vaillant M (2021) COVID-19 vaccine efficacy and effectiveness-the elephant (not) in the room. Lancet Microbe. https://doi.org/10.1016/S2666-5247(21)00069-0

Palese P, Young JF (1982) Variation of influenza A, B, and C viruses. Science 215(4539):1468–1474. https://doi.org/10.1126/science.7038875

Parton R, Hall E, Wardlaw AC (1994) Responses to Bordetella pertussis mutant strains and to vaccination in the coughing rat model of pertussis. J Med Microbiol 40(5):307–312. https://doi.org/10.1099/00222615-40-5-307

Paul S, Mahata A, Mukherjee S, Roy B, Salimi M, Ahmadian A (2022) Study of fractional order SEIR epidemic model and effect of vaccination on the spread of COVID-19. Int J Appl Comput Math 8(5):237. https://doi.org/10.1007/s40819-022-01411-4

Porco TC, Blower SM (1998) Designing HIV vaccination policies: subtypes and cross-immunity. Interfaces 28(3):167–190. https://doi.org/10.1287/inte.28.3.167

Porco TC, Blower SM (2000) HIV vaccines: the effect of the mode of action on the coexistence of HIV subtypes. Math Popul Stud 8(2):205–229. https://doi.org/10.1080/08898480009525481

Public Health England (2021) investigation-of-novel-sars-cov-2-variant-variant-of-concern-20201201. https://www.gov.uk/government/publications/investigation-of-novel-sars-cov-2-variant-variant-of-concern-20201201. Accessed 27 Sept 2021

Rahimi F, Abadi AT (2021) Implications of the emergence of a new variant of SARS-CoV-2, VUI-202012/01. Arch Med Res 52(5):569–571. https://doi.org/10.1016/j.arcmed.2021.01.001

Sansonetti PJ, Arondel J (1989) Construction and evaluation of a double mutant of Shigella flexneri as a candidate for oral vaccination against shigellosis. Vaccine 7(5):443–450. https://doi.org/10.1016/0264-410X(89)90160-6

Sato S, Suzuki K, Akahane Y, Akamatsu K, Akiyama K, Yunomura K, Tsuda F, Tanaka T, Okamoto H, Miyakawa Y, Mayumi M (1995) Hepatitis B virus strains with mutations in the core promoter in patients with fulminant hepatitis. Ann Intern Med 122(4):241–248. https://doi.org/10.7326/0003-4819-122-4-199502150-00001

Scherer A, McLean A (2002) Mathematical models of vaccination. Br Med Bull 62(1):187–199. https://doi.org/10.1093/bmb/62.1.187

Shastri J, Parikh S, Aggarwal V, Agrawal S, Chatterjee N, Shah R, Devi P, Mehta P, Pandey R (2021) Severe SARS-CoV-2 breakthrough reinfection with Delta variant after recovery from breakthrough infection by Alpha variant in a fully vaccinated health worker. Front Med 1:1379. https://doi.org/10.3389/fmed.2021.737007

Van den Driessche P, Watmough J (2002) Reproduction numbers and sub-threshold endemic equilibria for compartmental models of disease transmission. Math Biosci 180(1–2):29–48. https://doi.org/10.1016/S0025-5564(02)00108-6

Martcheva M (2014) Avian flu: modeling and implications for control. J Biol Syst 22(01):151–75. https://doi.org/10.1142/S0218339014500090

World Health Organization (2021a) https://covid19.who.int/region/searo/country/in. Accessed 29 Oct 2021

World Health Organization (2021b) https://covid19.who.int/. Accessed 29 Oct 2021

World Health Organization (2021c) WHO advisory committee on variola virus research: report of the thirteenth meeting report (World Health Organization, 2011). https://apps.who.int/iris/handle/10665/70778. Accessed 29 Oct 2021

World Health Organization (2021d) Tracking SARS-CoV-2 Variants. https://www.who.int/en/activities/tracking-SARS-CoV-2-variants/. Accessed 29 Oct 2021

Xue L, Jing SL, Wang H (2022) Evaluating the impacts of non-pharmaceutical interventions on the transmission dynamics of COVID-19 in Canada based on mobile network. PLoS ONE 16(12):e0261424. https://doi.org/10.1371/journal.pone.0261424

Yagan O, Sridhar A, Eletreby R, Levin S, Plotkin JB, Poor HV (2021) Modeling and analysis of the spread of COVID-19 under a multiple-strain model with mutations. Harvard Data Sci Rev 4:1. https://doi.org/10.1162/99608f92.a11bf693

Publisher's Note Springer Nature remains neutral with regard to jurisdictional claims in published maps and institutional affiliations.

Springer Nature or its licensor (e.g. a society or other partner) holds exclusive rights to this article under a publishing agreement with the author(s) or other rightsholder(s); author self-archiving of the accepted manuscript version of this article is solely governed by the terms of such publishing agreement and applicable law.